Localised Patterns in Continuum and Coupled-Cell Systems

Jonathan Dawes

Department of Mathematical Sciences
University of Bath

Outline

- Part IA - Magnetoconvection and *convectons*
- Part IB - Localised patterns in 1D continuum systems
  - the plain vanilla case
  - a new slant
- Part II - Localised patterns in 1D coupled cell systems
- Part III - From discrete to continuous
  - Model 6th order equation
  - Bifurcationology

J.H.P. Dawes, The emergence of a coherent structure for coherent structures: localized states in nonlinear systems. *Phil. Trans. Roy. Soc.* **368**, 3519–3534 (2010)
Special Issue: 'Visions of the future for the Royal Society's 350th anniversary year'.

Localised patterns - umbral dots

Bright points persist within the umbra of a sunspot

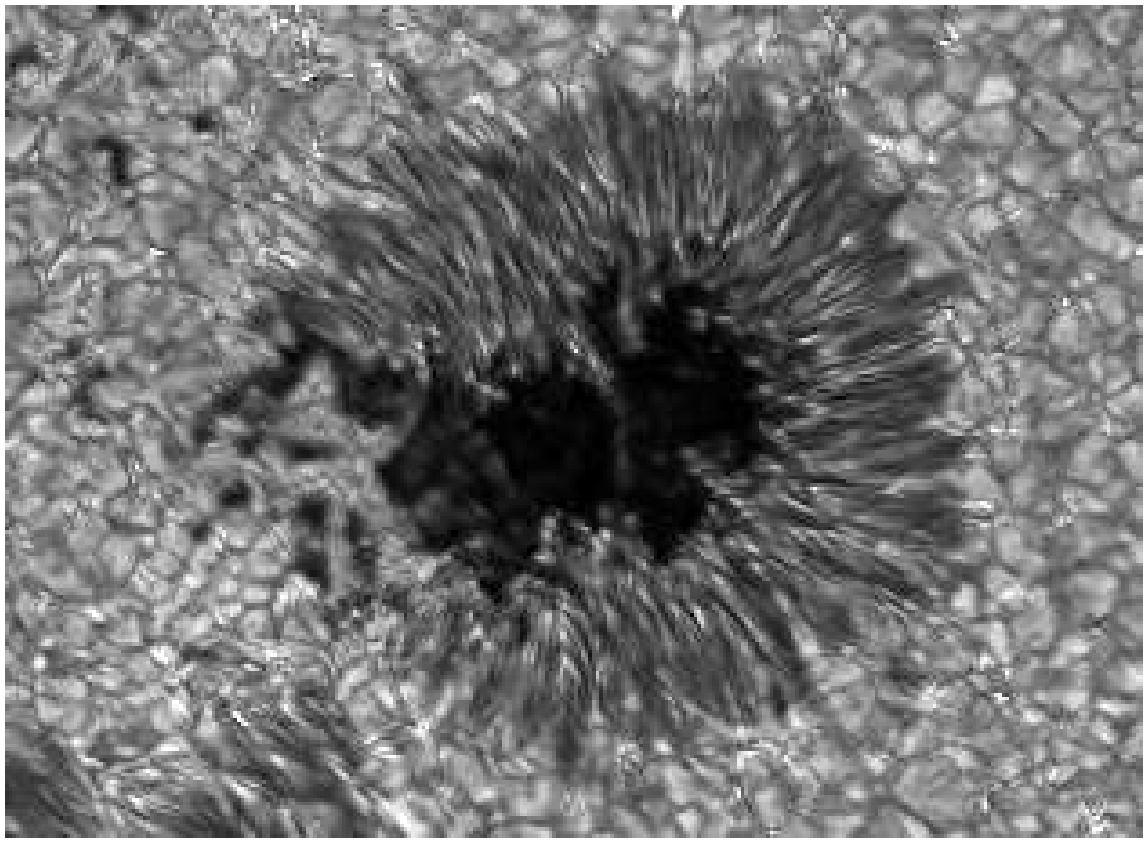

(AR 10786 imaged in the G Band, 8 June 2005)

Magnetoconvection

Numerical simulations: Rayleigh–Bénard convection with a vertical magnetic field

$R = 100000$, $Q = 1600$

$\sigma = 0.1$, $\zeta = 0.2$

stress-free, T fixed (lower)

radiative b.c. (upper)

$8 \times 8 \times 1$ stratified layer

density contrast approx 11.

blue = strong field

purple = weak field

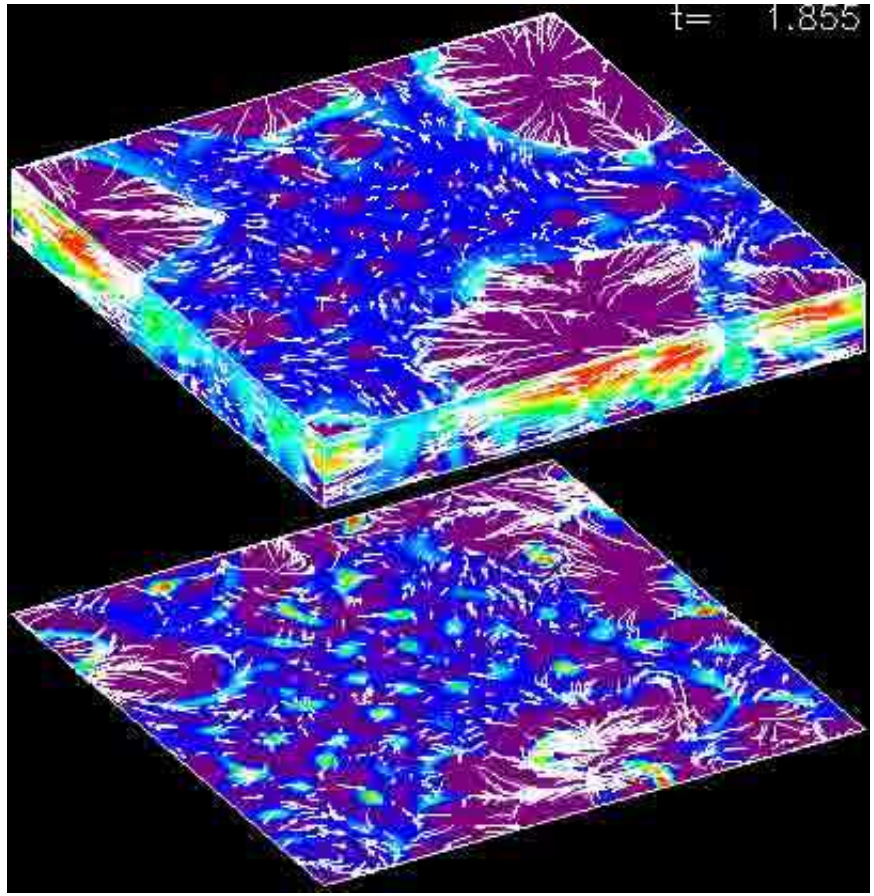

A.M. Rucklidge, N.O. Weiss, D.P. Brownjohn, P.C. Matthews & M.R.E. Proctor, *J. Fluid Mech.* **419**, 283–323 (2000)

Localised magnetoconvection

$$R = 20\,000,\ Q = 14\,000,\ \zeta = 0.1,\ \sigma = 1.0,\ L = 6.0$$

Temperature (deviation) & velocity:

$|\mathbf{B}|^2$:

Subcritical finite-amplitude magnetoconvection noted by several previous authors:

- N.O. Weiss *Proc. Roy. Soc. Lond.* (1966) – flux expulsion
- F.H. Busse, *J. Fluid Mech.* **71** 193–206 (1975):

  "...thus finite amplitude onset of steady convection becomes possible at Rayleigh numbers considerably below the values predicted by linear theory."

Puzzle: convection cells persist even at very high field strengths

Localised magnetoconvection

- Strongly nonlinear localised states (‘convectons’) persist for strong fields.
- $\frac{dT}{dz}|_{\rm top}$ for increasing Q at fixed R:

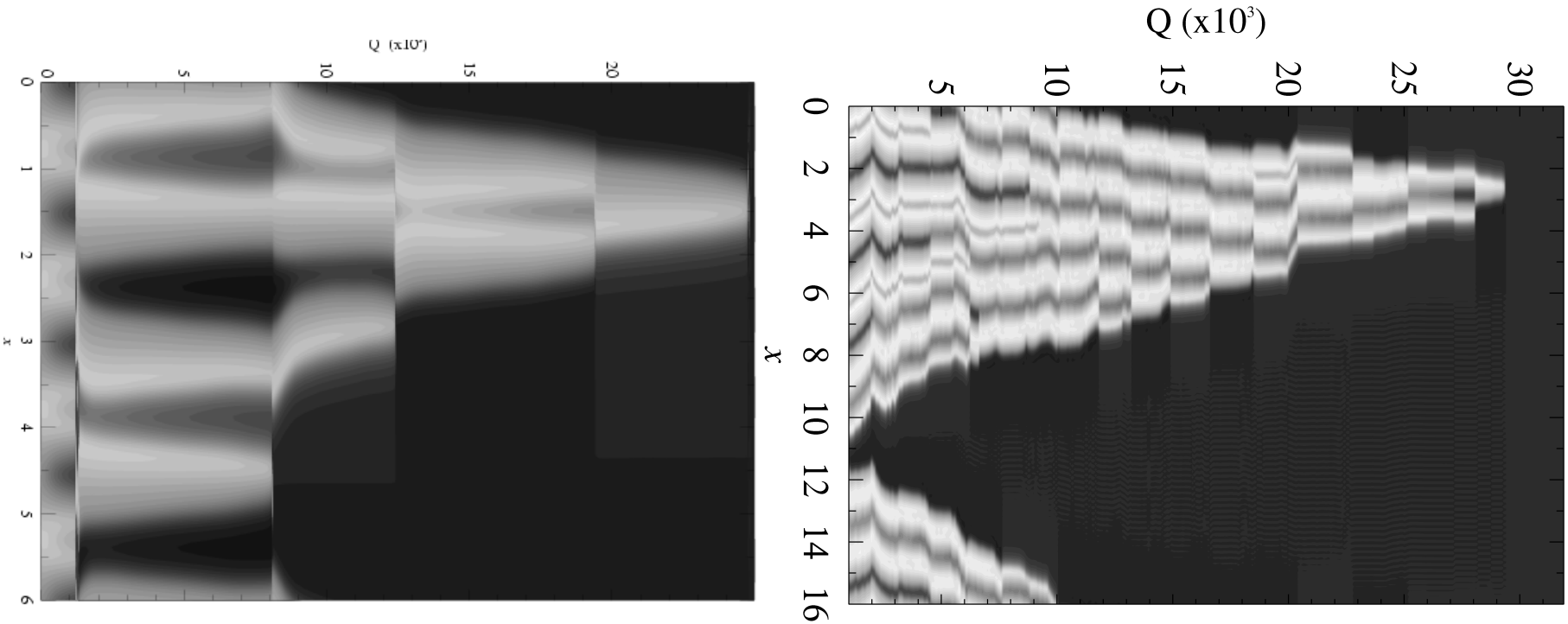

S.M. Blanchflower, *Phys. Lett.* A **261**, 74–81 (1999); PhD thesis, University of Cambridge (1999)

- What is the connection with linear (and weakly nonlinear) theory ??

Part IB
Patterns in 1D continuum systems

Pattern formation in the lab

Rayleigh–Bénard convection

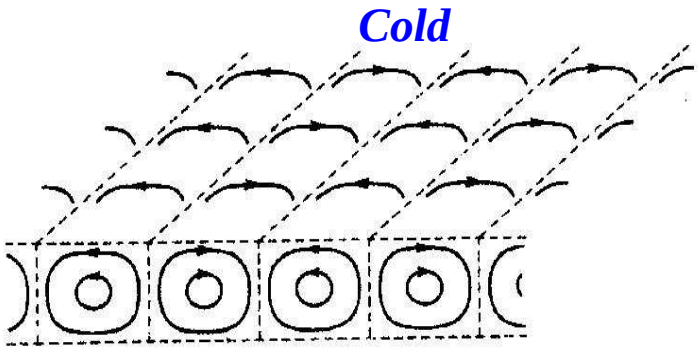

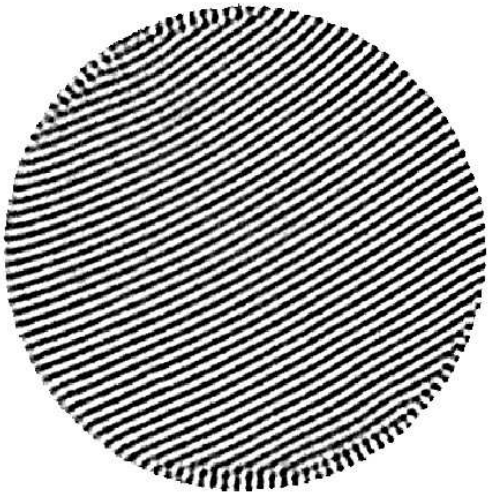

Ideal Straight Rolls

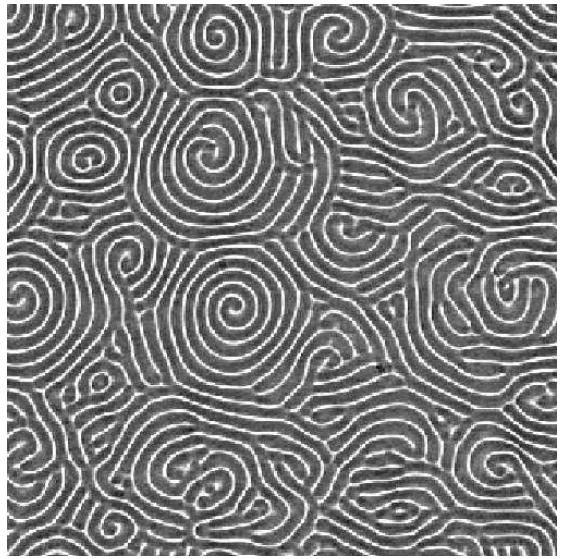

Spiral Defect Chaos

S.W. Morris, E. Bodenschatz, D.S. Cannell and G. Ahlers *Phys. Rev. Lett.* **71**, 2026–2029 (1993)

Pattern formation in the lab

Faraday waves (2-frequency forcing, harmonic response)

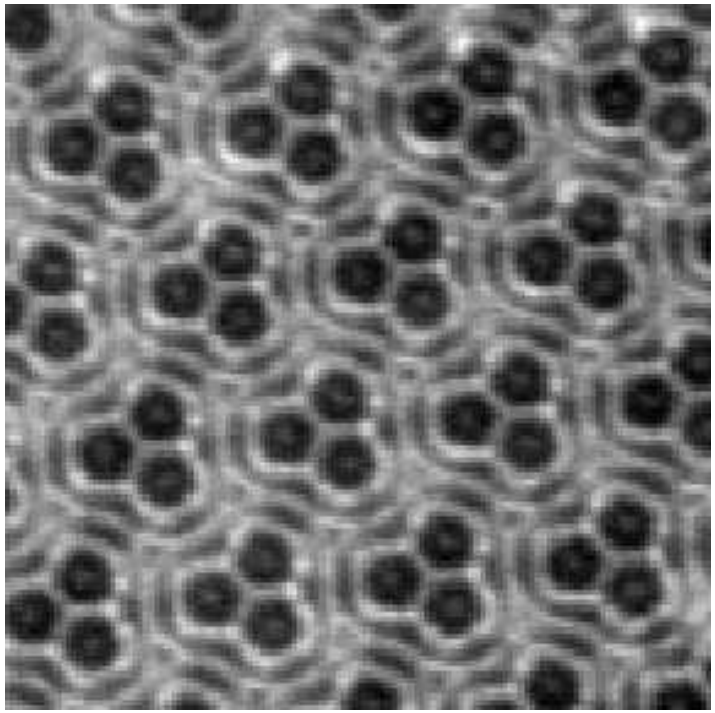

Superlattice (‘down’) triangles

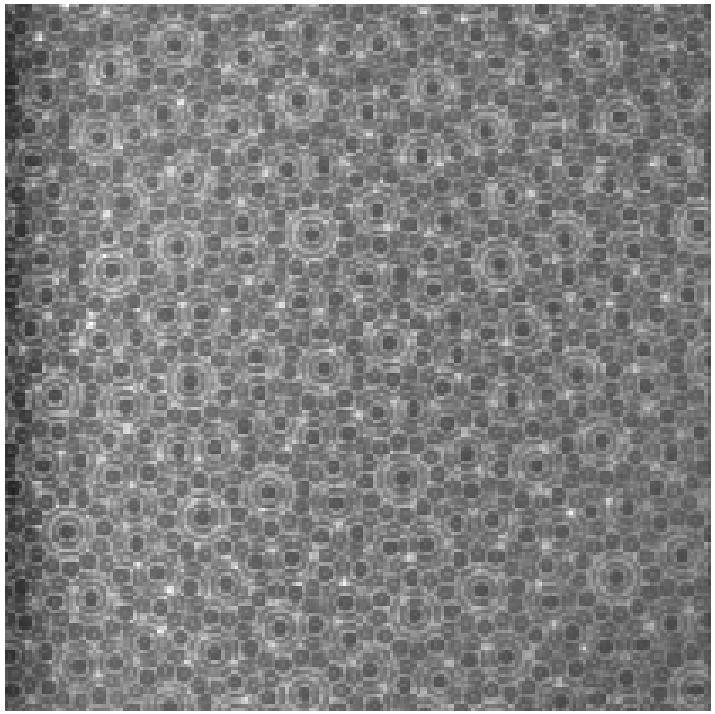

12-fold quasiperiodic pattern

A. Kudrolli, B. Pier & J.P. Gollub *Physica* D **123**, 99–111 (1998)
M. Silber & M.R.E. Proctor *Phys. Rev. Lett.* **81**, 2450–2453 (1998)

Localised pattern formation

Granular and viscoelastic Faraday experiments

Granular ‘oscillons’

Viscoelastic ’holes’

P.B. Umbanhowar, F. Melo and H.L. Swinney, *Nature* **382**, 793 (1996)
F. Merkt, R.D. Deegan, D. Goldman, E. Rericha, and H.L. Swinney, *Phys. Rev. Lett.* **98**, 184501 (2004)
J.H.P. Dawes & S. Lilley, *SIAM J. Appl. Dyn. Syst.* **9**, 238–260 (2010)

Simple models for pattern formation

Suppose system state is described by a scalar variable $w(x,t)$, $x \in \mathbb{R}$.

'Turing instability' from trivial state to patterned state occurs.

Assume

- translational symmetry $x \to x + \delta$
- reflectional symmetry $x \to -x$
- unbounded domain: $-\infty < x < \infty$
  (replaced with periodic boundaries (PBC) in practice)

Eigenfunctions: plane waves $\mathrm{e}^{\mathrm{i}kx}$; steady state instability at $|k| = 1$:

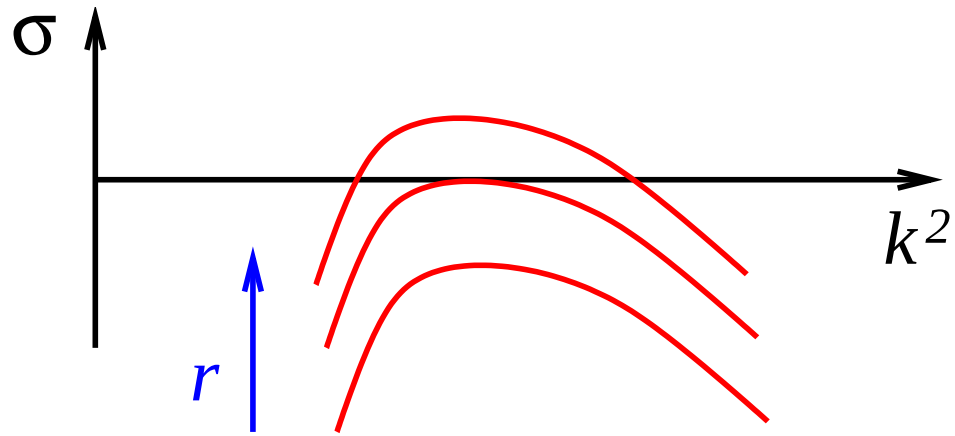

Growth rate: $\sigma = r - (1 - k^2)^2$

Swift–Hohenberg equation

$$\partial_t w = [r - (1 + \partial_{xx}^2)^2]w + N(w)$$

Nonlinearities:

- $-w^3$ – supercritical ('forwards') bifurcation
- $+bw^2 - w^3$, $+sw^3 - w^5$ – subcritical ('backwards') bifurcations

Near bifurcation point, $r = \varepsilon^2 \mu$, there is a band of unstable modes:

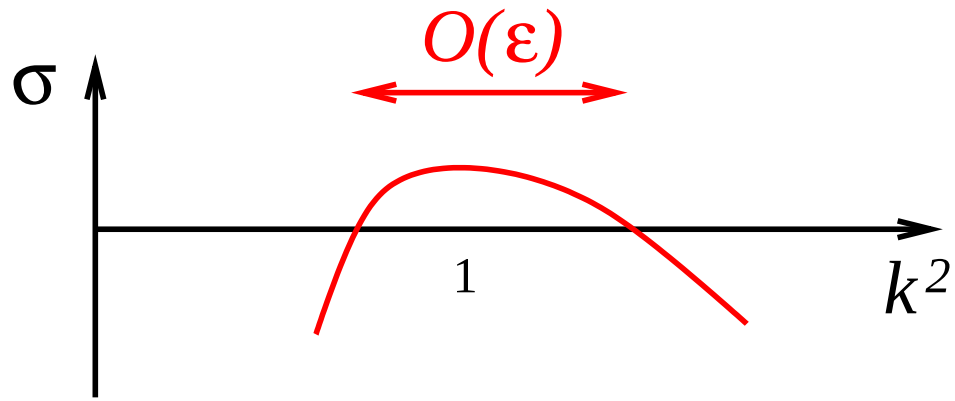

- Finite domain with PBC allows only a discrete set of modes
- on $\mathbb{R}$ no centre manifold reduction is formally possible

Ginzburg–Landau approach

Suppose the pattern-forming instability is weakly subcritical and symmetric: $w \to -w$.

Model equation: $w_t = [r - (1 + \partial_{xx}^2)^2]w + sw^3 - w^5$

Asymptotic scalings for a weakly subcritical bifurcation:

$$w(x,t) \quad = \quad \varepsilon \left(A(X,T)\mathrm{e}^{\mathrm{i}x} + c.c. \right) + \varepsilon^2 w_2 + \cdots$$

$s = \varepsilon^2 \hat{s} \qquad X = \varepsilon^2 x, \qquad T = \varepsilon^4 t, \qquad r = \varepsilon^4 \hat{r}$

At $O(\varepsilon^5)$ we deduce

$$\boxed{A_T = \hat{r}A + 4A_{XX} + 3\hat{s}A|A|^2 - 10A|A|^4}$$

Now drop hats, and examine instability to perturbations $\mathrm{e}^{\mathrm{i}\ell X}$.

Modulational instability

Monotonic branch of modulated pattern bifurcates:

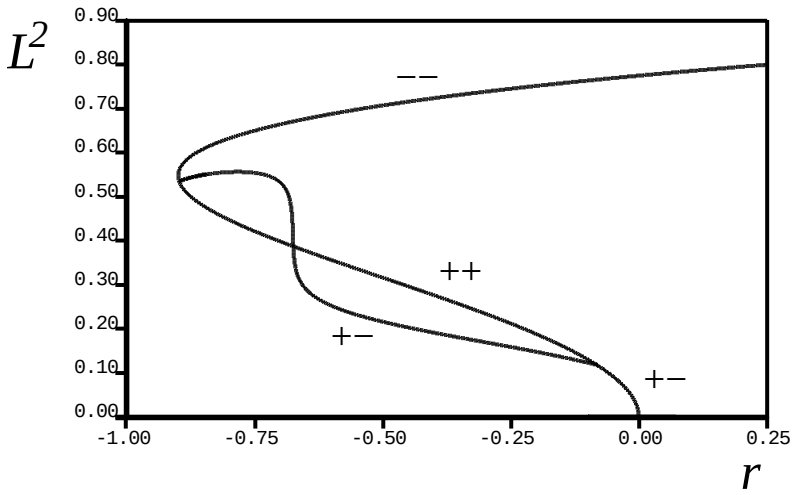

$0 \leq X \leq 10\pi$

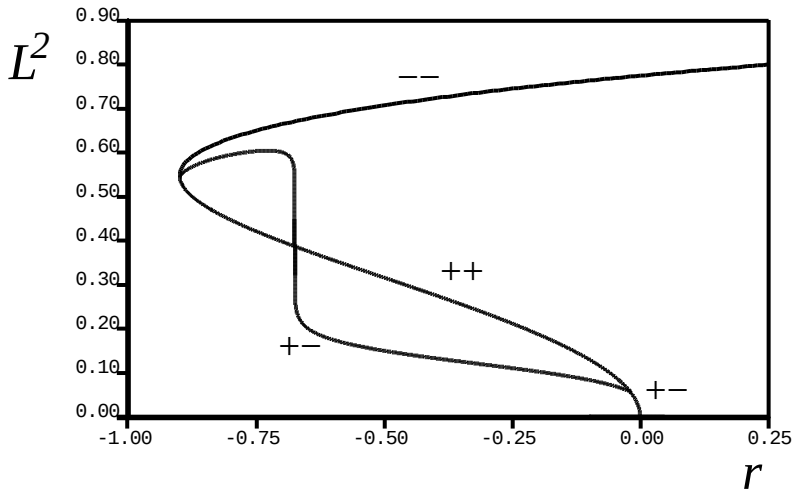

$0 \leq X \leq 20\pi$

First integral ('energy'): $E = \frac{r}{2}A^2 + 2(A_X)^2 + \frac{3s}{4}A^4 - \frac{5}{3}A^6$

Maxwell point at $r = r_{mx}$, defined by $E|_{A=0} = E|_{A=A_0^+}$ – stationary fronts exist.

Maxwell point: $E|_{A=0} = E|_{A=A_0^+}$ when $r = -0.675$.

Homoclinic snaking - finite domain

Return to Swift–Hohenberg equation: $w_t = [r - (1 + \partial_{xx}^2)^2]w + sw^3 - w^5$.
Fix $s = 2.0$ and domain size $L = 10\pi$ (PBC).

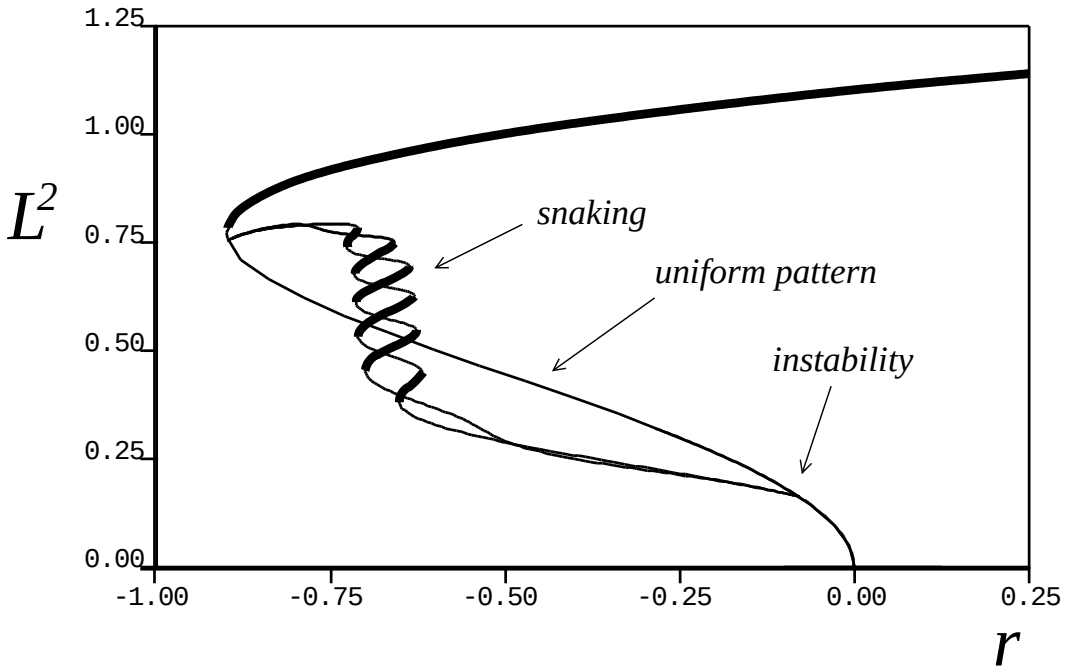

Odd:

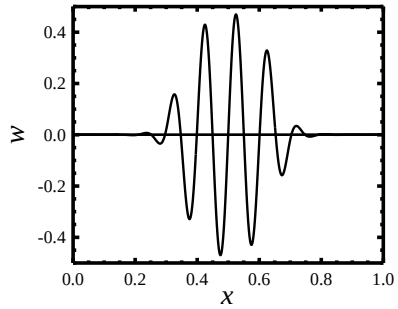

Even:

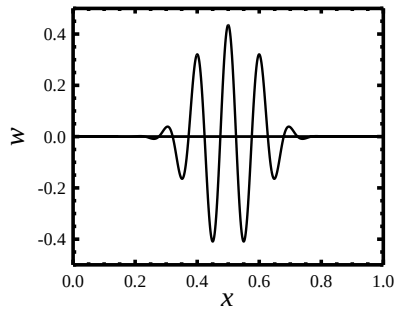

- Modulational instability produces localised states
- Cross-link, or ‘ladder’ branches also exist

Spatial dynamics

Think of x as 'time' variable and look for steady states:

$$0 \quad = \quad (r-1)w - 2w_{xx} - w_{xxxx} - N(w)$$

4D reversible dynamical system: $U = w$, $V = w_x$, $W = w_{xx}$, $Z = w_{xxx}$

$$\begin{pmatrix} U \\ V \\ W \\ Z \end{pmatrix}_x = \begin{pmatrix} 0 & 1 & 0 & 0 \\ 0 & 0 & 1 & 0 \\ 0 & 0 & 0 & 1 \\ r-1 & 0 & -2 & 0 \end{pmatrix} \begin{pmatrix} U \\ V \\ W \\ Z \end{pmatrix} - N(U, V, W, Z)$$

Eigenvalues at bifurcation point are $\pm \mathrm{i}$, twice each:

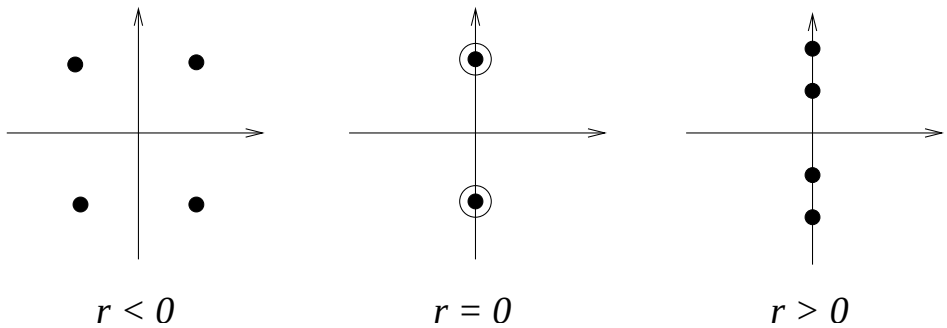

'Hamiltonian–Hopf' bifurcation

Homoclinic tangle

Interpret as dynamics of a map on a Poincaré section:

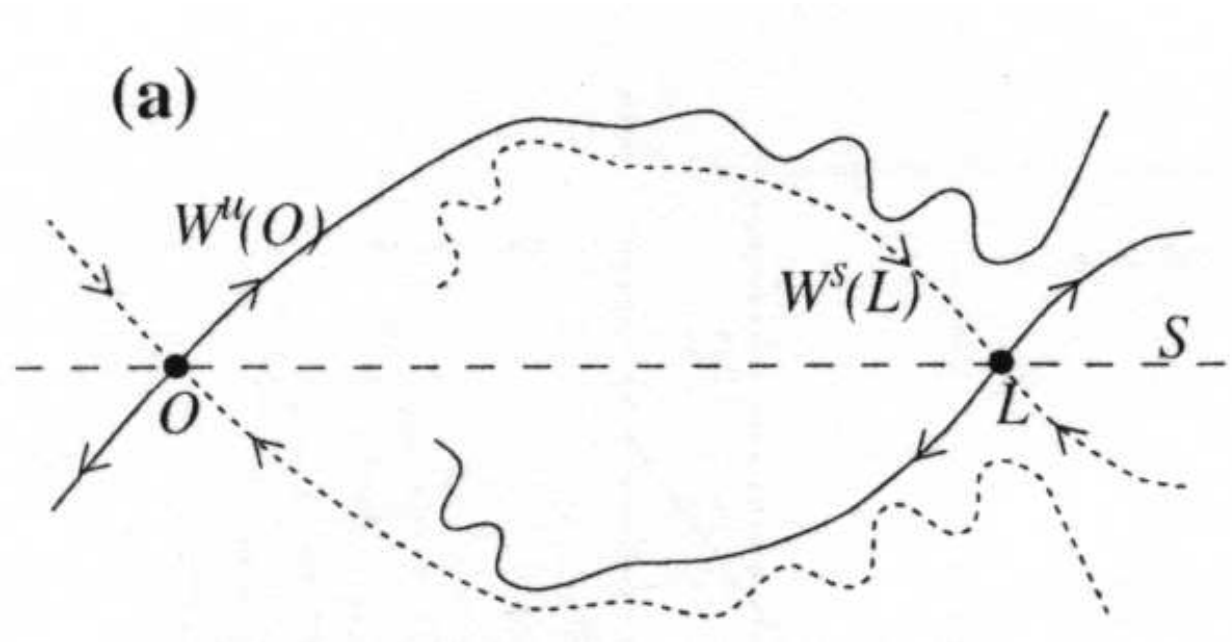

Homoclinic tangle

Interpret as dynamics of a map on a Poincaré section:

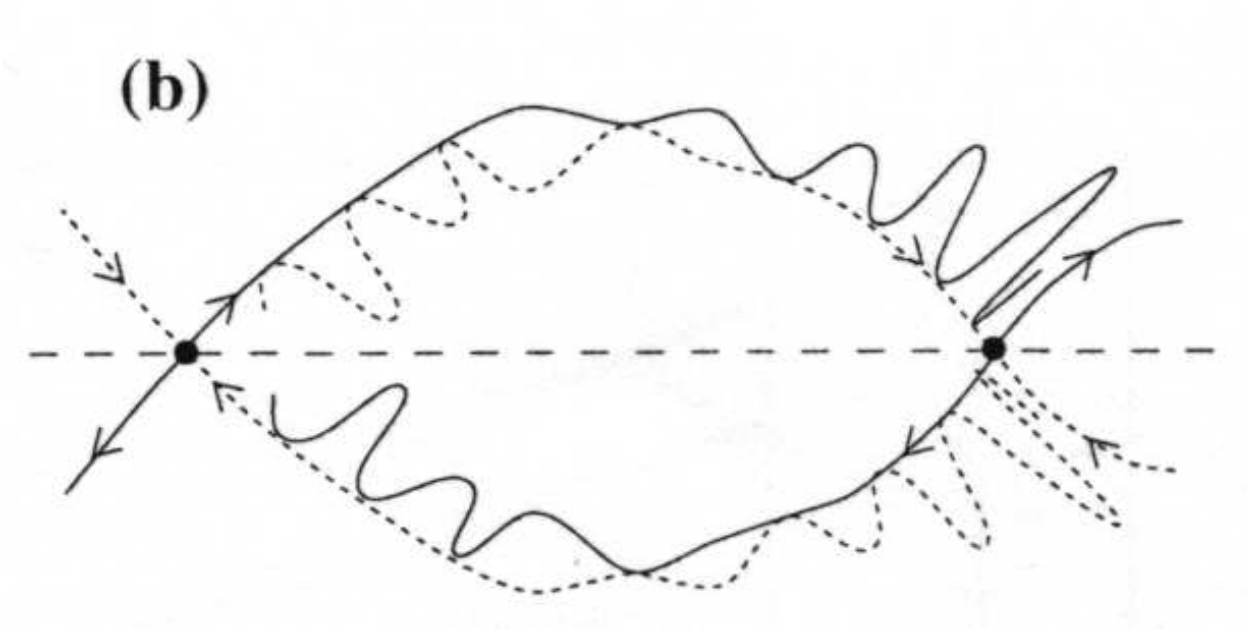

Homoclinic tangle

Interpret as dynamics of a map on a Poincaré section:

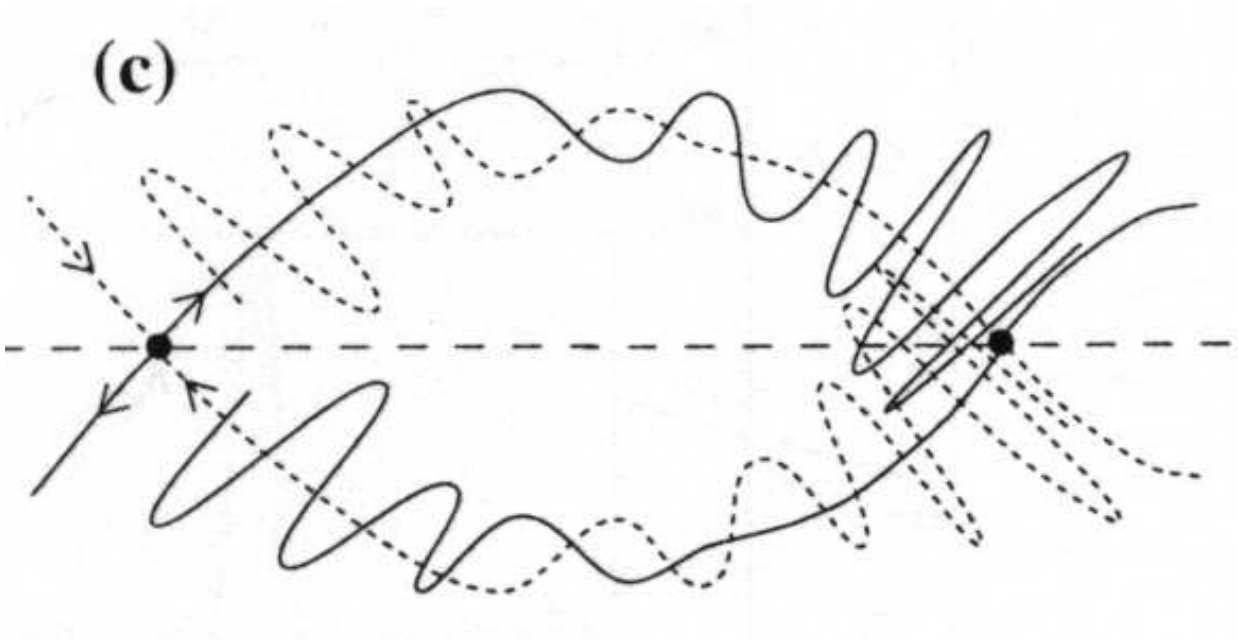

Homoclinic tangle

Interpret as dynamics of a map on a Poincaré section:

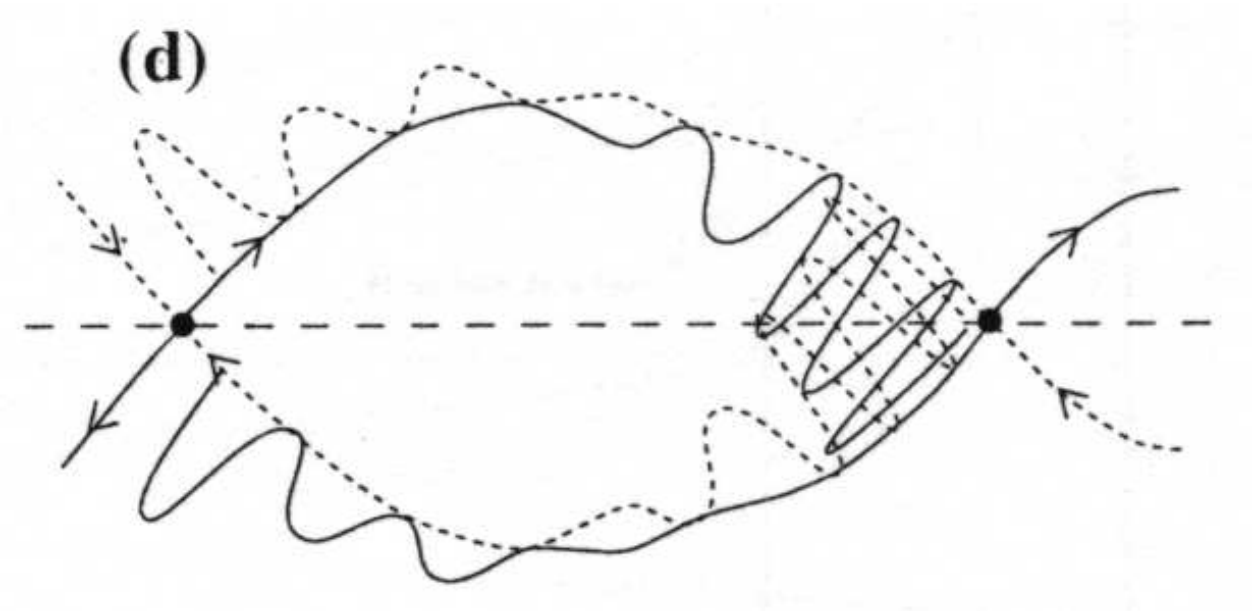

Homoclinic tangle

Interpret as dynamics of a map on a Poincaré section:

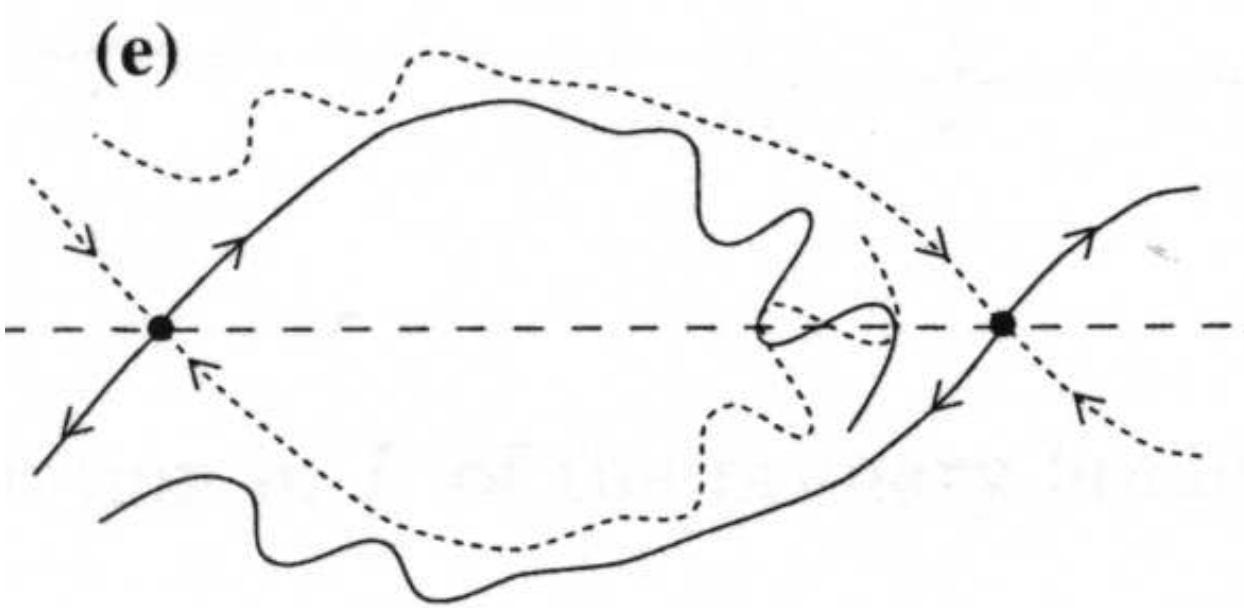

Homoclinic tangle

Interpret as dynamics of a map on a Poincaré section:

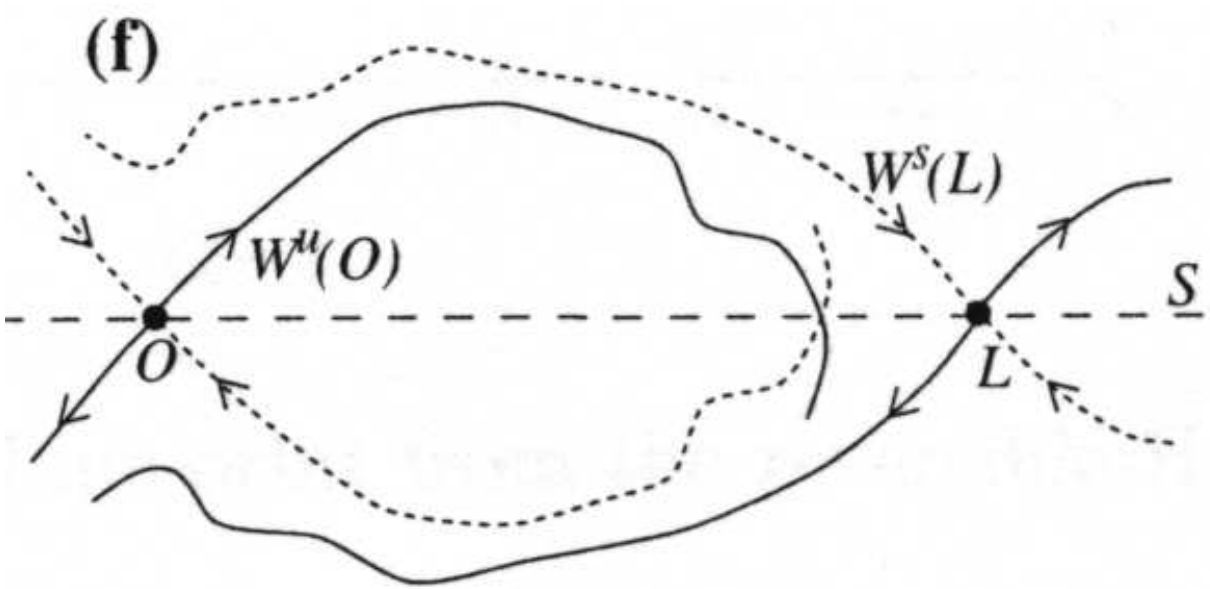

Homoclinic snaking

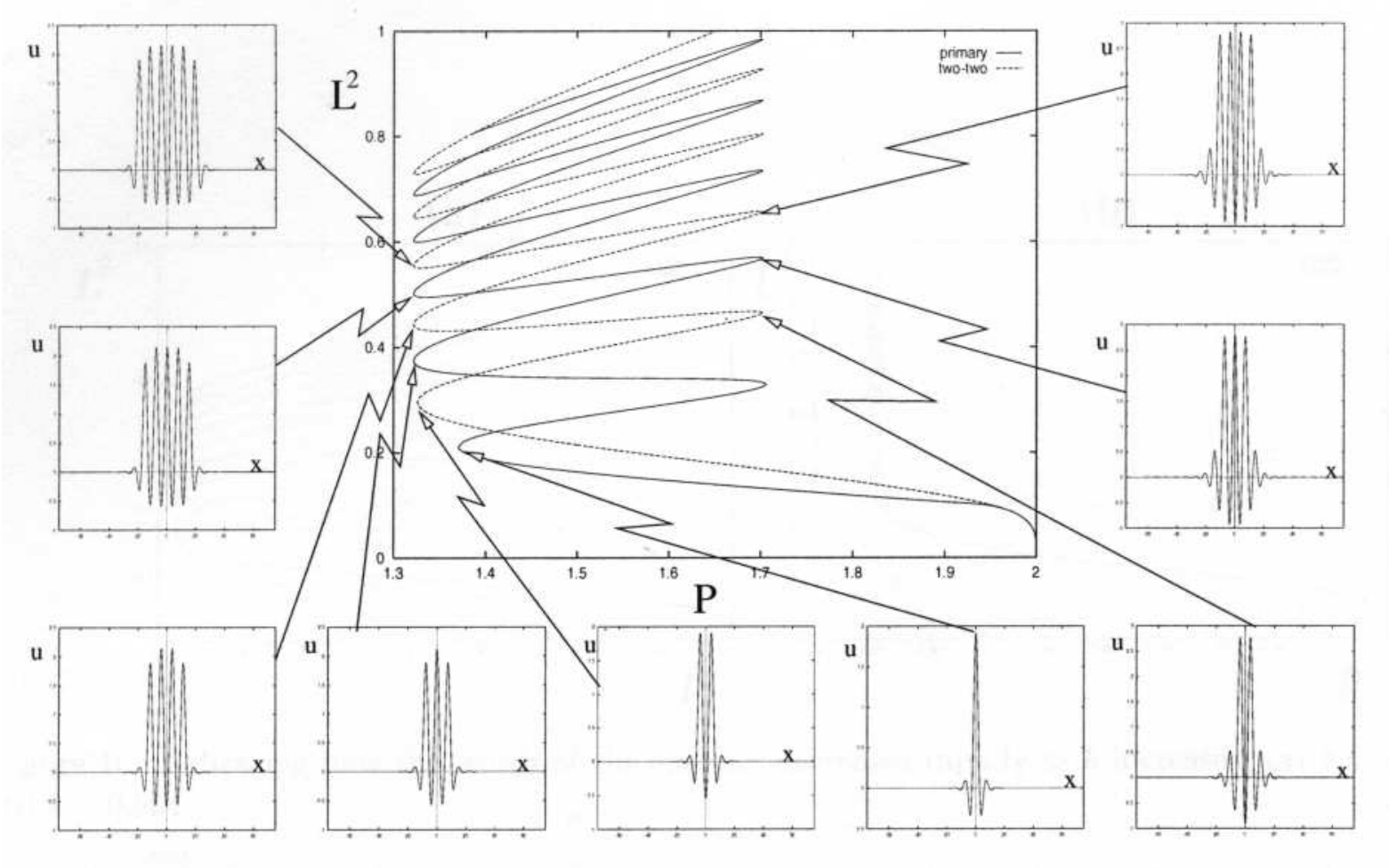

$$0 = w + Pw_{xx} + w_{xxxx} - w^2 + 0.3w^3$$

P.D. Woods and A.R. Champneys *Physica* D **129**, 147 (1999)

Magnetoconvection: model problem

$$w_t = [r - (1 + \partial_{xx}^2)^2]w - w^3 - QB^2 w \qquad (1)$$
$$B_t = \zeta B_{xx} + \tfrac{1}{\zeta}(w^2 B)_{xx} \qquad (2)$$

Symmetries:

- $w \to -w$ (Boussinesq problem)
- $B \to -B$ (direction of magnetic field)

Parameters:

- r - reduced Rayleigh number $r = R/R_c$
- Q - Chandrasekhar number $\propto |B_0|^2$
- $\langle B \rangle = 1$ after nondimensionalising
- ζ - magnetic/thermal diffusivity ratio $\zeta = \eta/\kappa$

Remark: We could do a weakly nonlinear analysis, writing

$$w = \varepsilon w_1 + \cdots, \qquad B = 1 + \varepsilon^2 B_2 + \cdots, \qquad X = \varepsilon x, \qquad T = \varepsilon^2 t$$

– the scaling introduced by Matthews & Cox.

P.C. Matthews & S.M. Cox *Nonlinearity* **13**, 1293–1320 (2000)

Magnetoconvection: model problem

Set $\partial_t \equiv 0$. Integrate (2) twice:

$$\zeta P \quad = \quad B\left(\zeta + \frac{w^2}{\zeta}\right)$$

where P is a constant of integration.

Re-arrange and integrate over the domain $[0, L]$: $\left\langle \frac{P}{1+w^2/\zeta^2} \right\rangle = \langle B \rangle \stackrel{\text{def}}{=} 1$

Hence

$$\frac{1}{P} \quad = \quad \left\langle \frac{1}{1 + w^2/\zeta^2} \right\rangle$$

So $P[w]$ measures the higher concentration of the large-scale mode in the region *outside* the localised pattern. Substituting, we obtain

$$0 \quad = \quad [r - (1 + \partial_{xx}^2)^2]w - w^3 - \frac{QP^2 w}{(1 + w^2/\zeta^2)^2}$$

Nonlocal Ginzburg–Landau eqn

$$0 \quad = \quad [r - (1 + \partial_{xx}^2)^2]w - w^3 - \frac{QP^2 w}{(1 + w^2/\zeta^2)^2}$$

- Suppose $\zeta \ll 1$
- Introduce the long scales $X = \zeta x$, $T = \zeta^2 t$.
- Rescale: $Q = \zeta^2 q$ and $r = \zeta^2 \mu$.
- Expand: $w(x,t) = \zeta A(X,T) \sin x + O(\zeta^2)$, assuming $A(X,T)$ real.

Interpret spatial average as over both $x \in [0, 2\pi]$ and X:

$$\frac{1}{P} = \left\langle \left\langle \frac{1}{1 + A^2 \sin^2 x} \right\rangle_x \right\rangle_X = \left\langle \frac{1}{\sqrt{1 + A^2}} \right\rangle_X$$

Extract solvability condition by multiplying by $\sin x$ and integrating over x:

$$0 \quad = \quad \mu A + 4A_{XX} - 3A^3 - \frac{qP^2 A}{(1 + A^2)^{3/2}}$$

Return to (w, B) equations

$$w_t = [r - (1 + \partial_{xx}^2)^2]w - w^3 - QB^2w \qquad (1)$$
$$B_t = \zeta B_{xx} + \tfrac{1}{\zeta}(w^2 B)_{xx} \qquad (2)$$

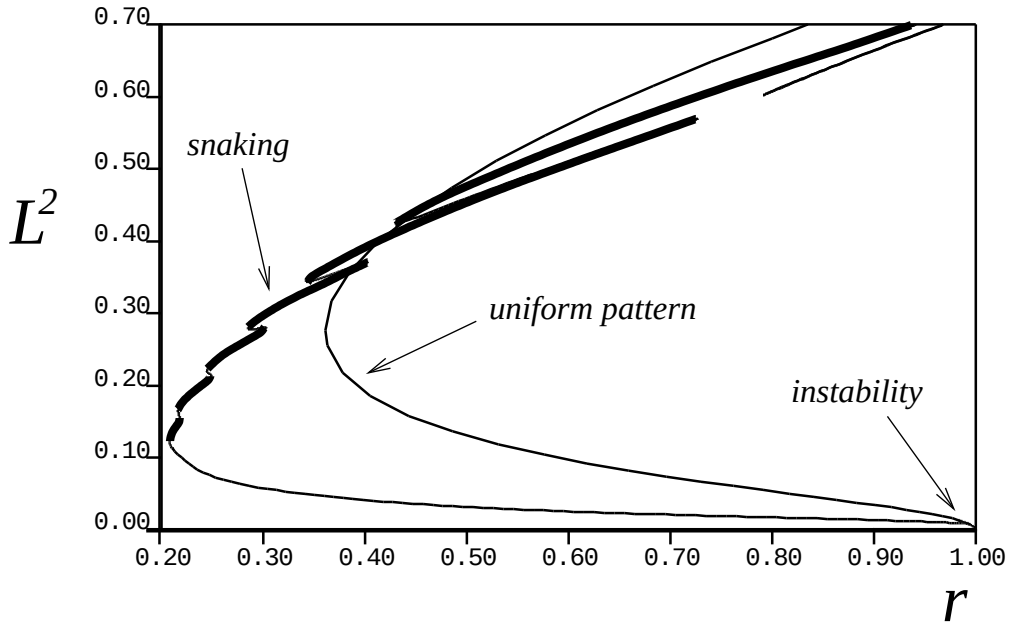

Slanted snaking

J.H.P. Dawes, Localised pattern formation with a large-scale mode: slanted snaking. *SIAM J. App. Dyn. Syst.* **7**, 186–206 (2008)

Locations of saddle-nodes

Full magnetoconvection equations:

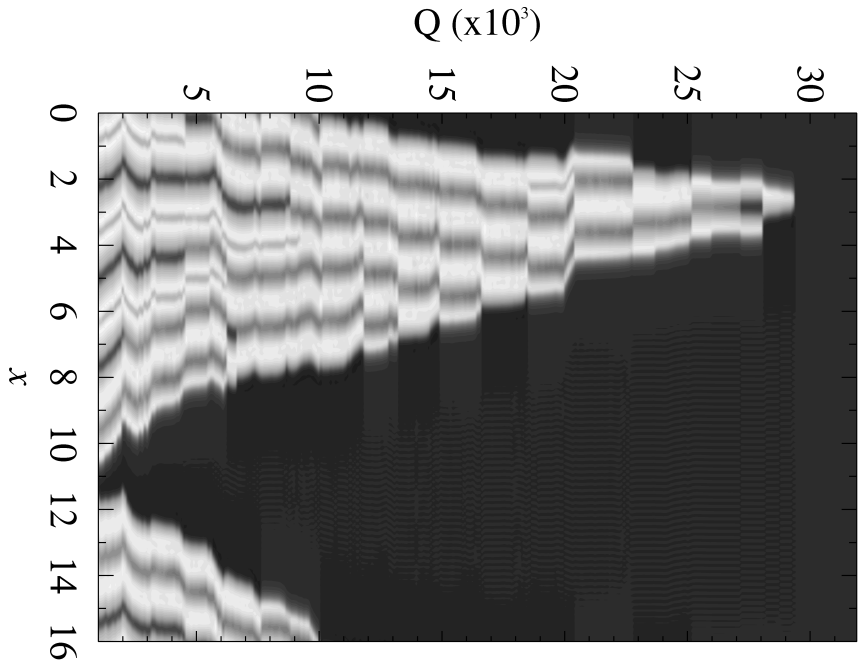

Toy model:

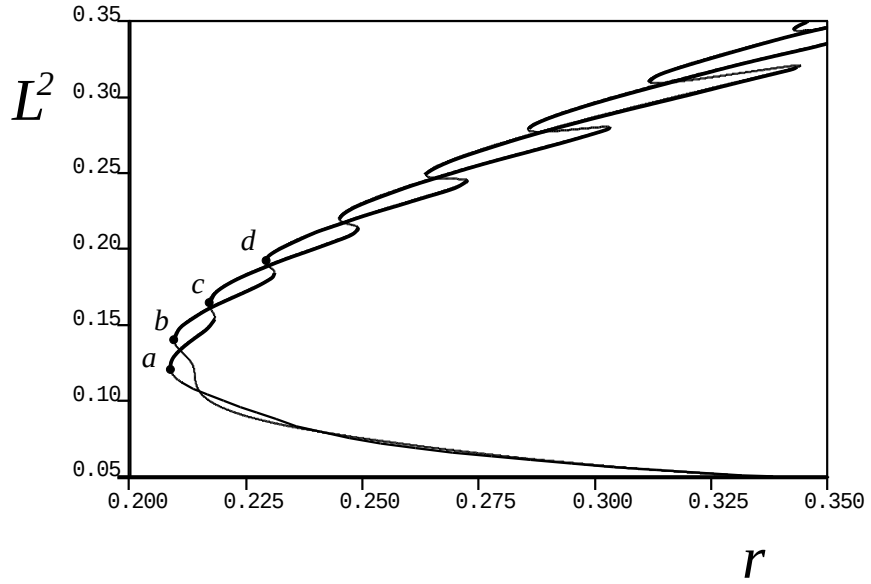

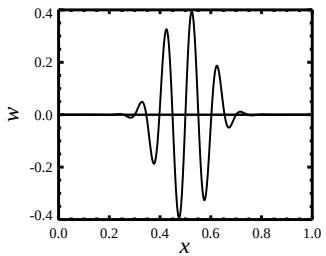

(a)

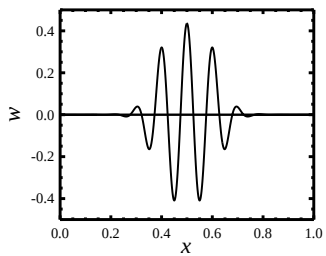

(b)

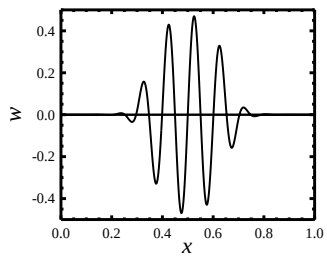

(c)

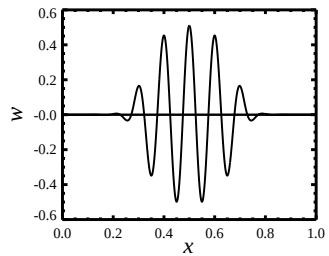

(d)

Part II
Localised patterns in 1D coupled cell systems

Example: juxtacrine cell signalling

- Juxtacrine (cell-to-cell) signalling is important in embryonic development, e.g. delta-notch signalling in zebrafish segmentation:

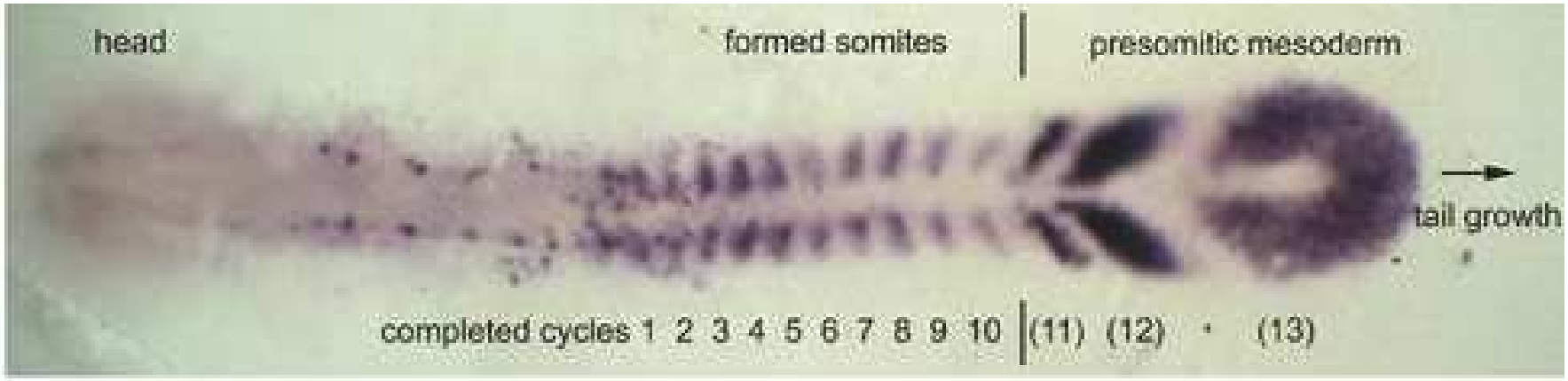

- Between cells: delta activates notch
- Within a cell: notch deactivates delta

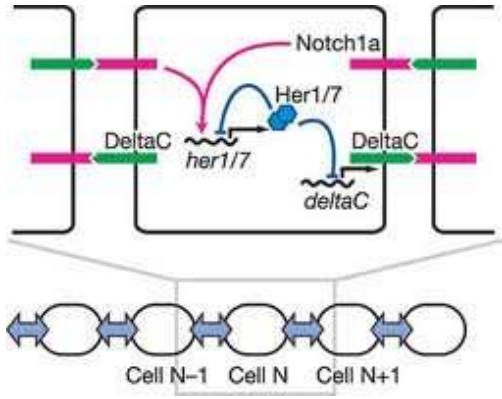

- Signalling may enhance differences between neighbouring cells, rather than suppressing them.

Example: juxtacrine cell signalling

- Often leads to the formation of (periodic) spatial patterns and fronts:

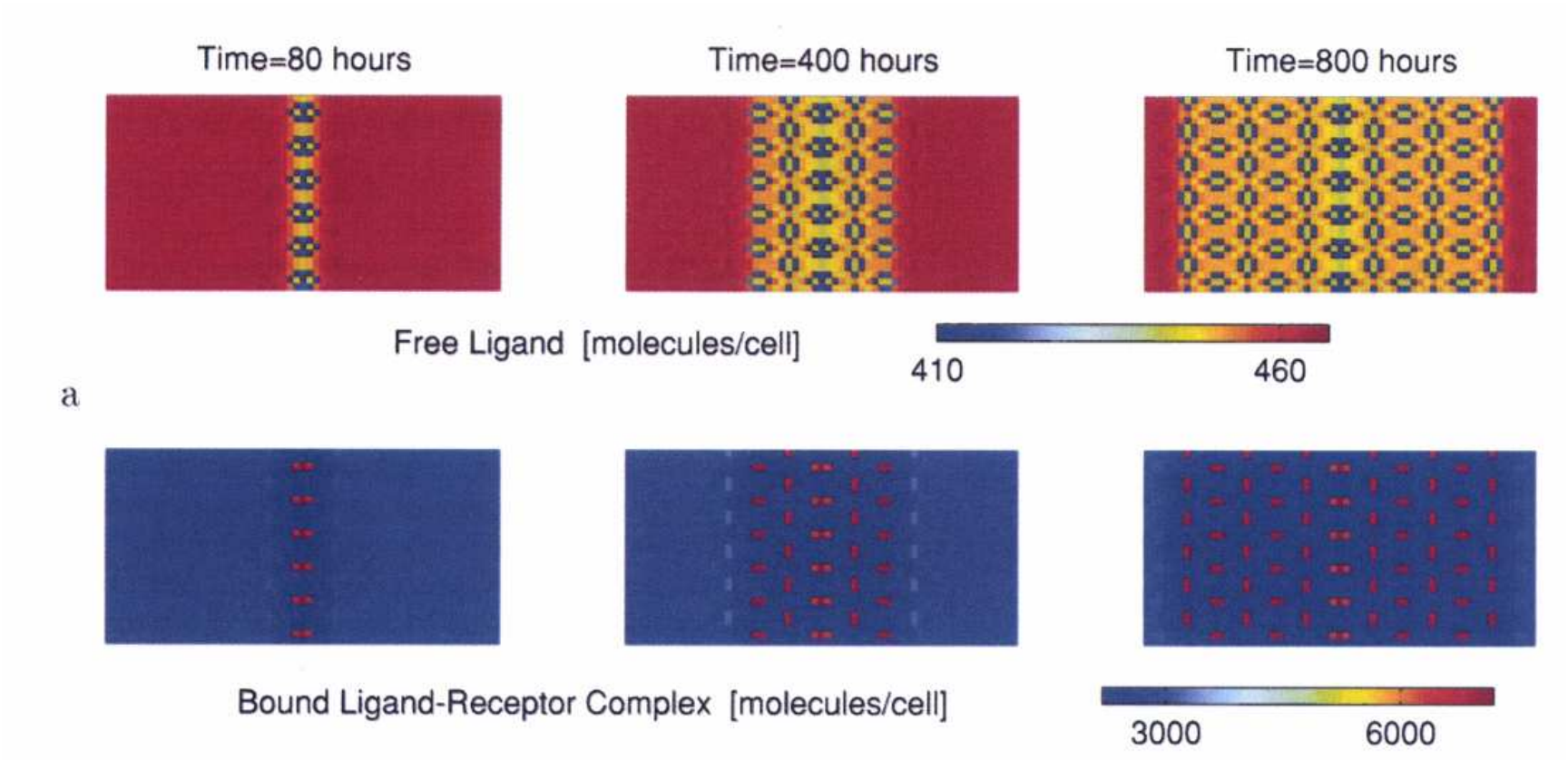

M.R. Owen, J.A. Sherratt & H.J. Wearing, *Developmental Biology* **217**, 54–61 (2000)
J.R. Collier, N.A.M. Monk, P.K. Maini & J.H. Lewis *J. Theor. Biol.* **183**, 429–446 (1996)

Example: juxtacrine cell signalling

- ... or localised patterns of activity:

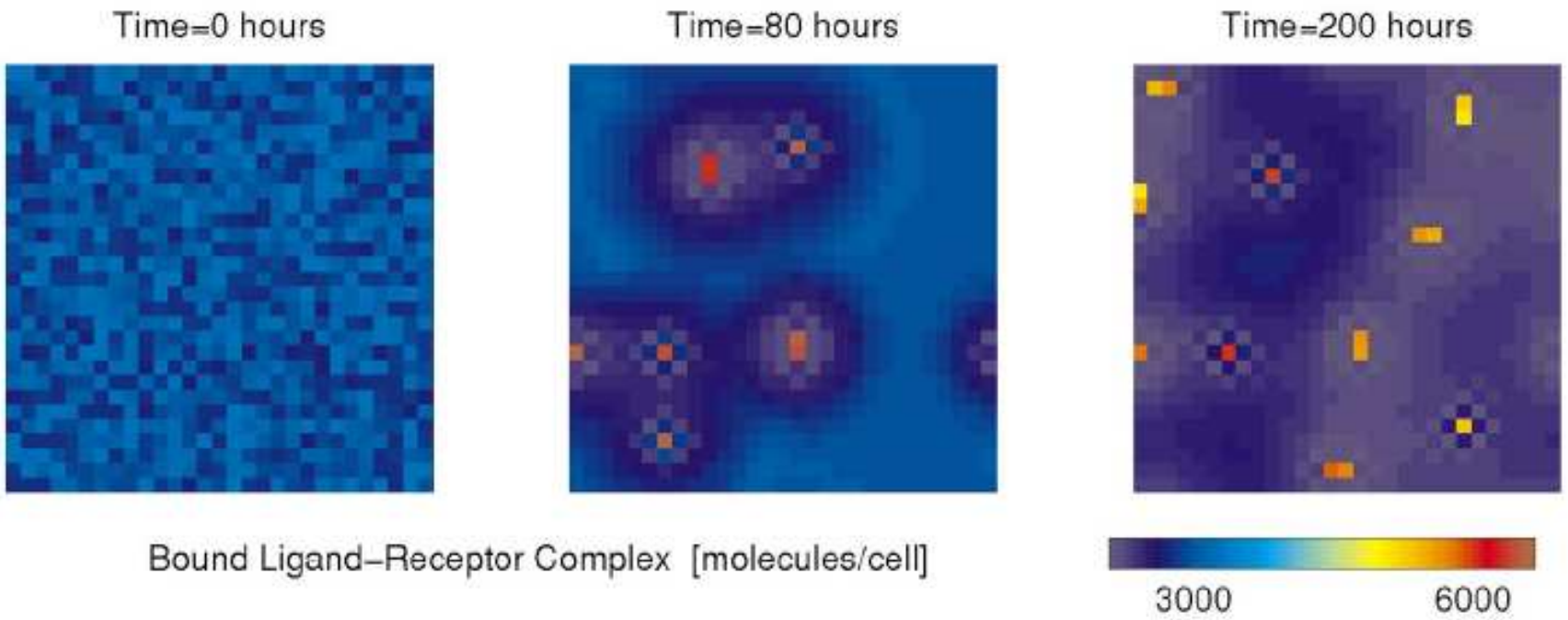

Model equation in 1D

- ‘Spatially discrete bistable Allen–Cahn equation’:

$$(\dot{u}_n) \qquad 0 = C(u_{n+1} - 2u_n + u_{n-1}) + \mu u_n + 2su_n^3 - u_n^5$$

- Motivated by the discrete nonlinear Schrödinger equation:

$$\mathrm{i}\dot{\psi}_n + C(\psi_{n+1} - 2\psi_n + \psi_{n-1}) + 2s\psi_n|\psi_n|^2 - \psi_n|\psi_n|^4 = 0$$

after substituting $\psi_n(t) = u_n \exp(-\mathrm{i}\mu t)$.

- describes dynamics of a periodic array of optical cavities driven by a coherent light source:

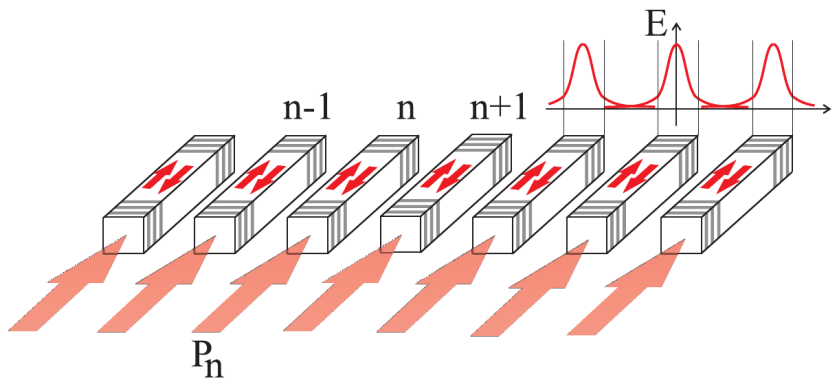

A.V. Yulin, A.R. Champneys & D.V. Skryabin, Discrete cavity solitons due to saturable nonlinearity *Phys. Rev.* A **78**, 011804 (2008)

Localised states in 1D

- Localised states exist on snaking curves:

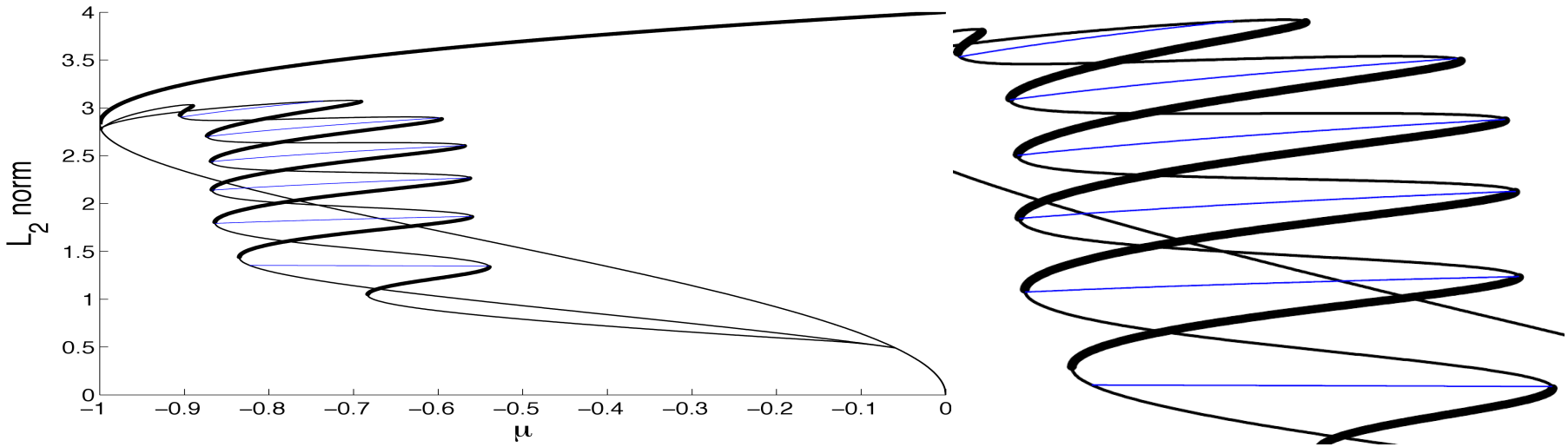

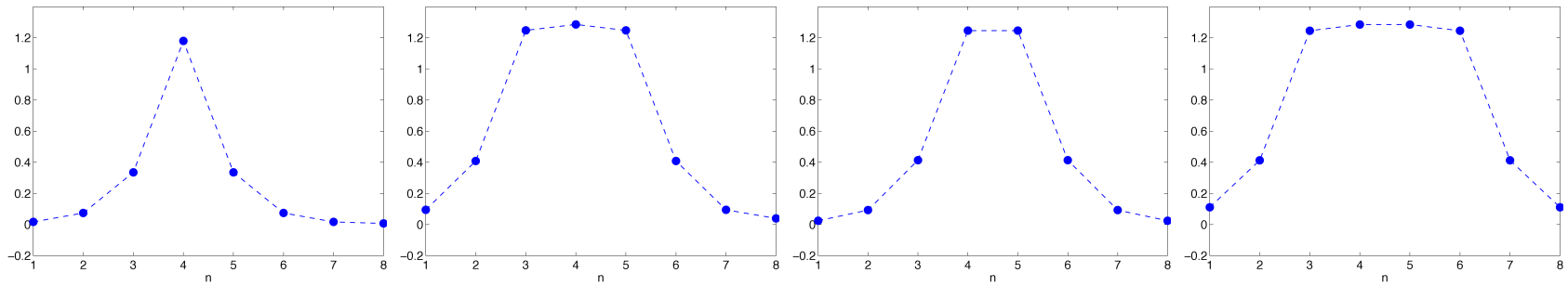

site-centred

bond-centred

C.R.N. Taylor & J.H.P. Dawes, Snaking and isolas of localized states in bistable discrete lattices. Preprint (2009)

Digression into 2D

- Natural extensions of 1D couplings are:

$$\begin{aligned}\Delta^{+}u_{n\,m} &= u_{n+1\,m} + u_{n-1\,m} + u_{n\,m+1} + u_{n\,m-1} - 4u_{n\,m}\\ \Delta^{\times}u_{n\,m} &= u_{n+1\,m+1} + u_{n-1\,m+1} + u_{n+1\,m-1} + u_{n-1\,m-1} - 4u_{n\,m}\end{aligned}$$

- $\Rightarrow$ Allen–Cahn equation generalises to

$$(\dot{u}_{nm})\ 0 = C^{+}\Delta^{+}u_{nm} + C^{\times}\Delta^{\times}u_{nm} + \mu u_{nm} + 2su_{nm}^{3} - u_{nm}^{5}$$

- In 2D there are three types of localised state:

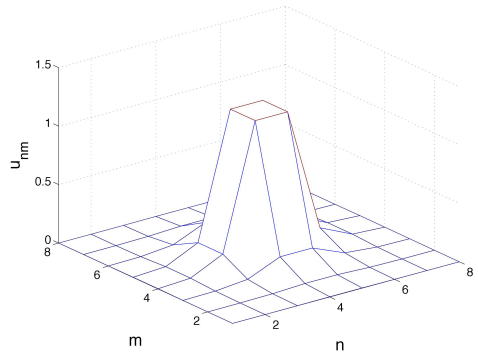

bond-centred

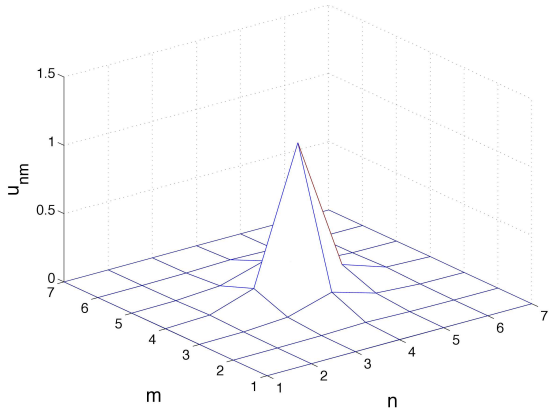

site-centred

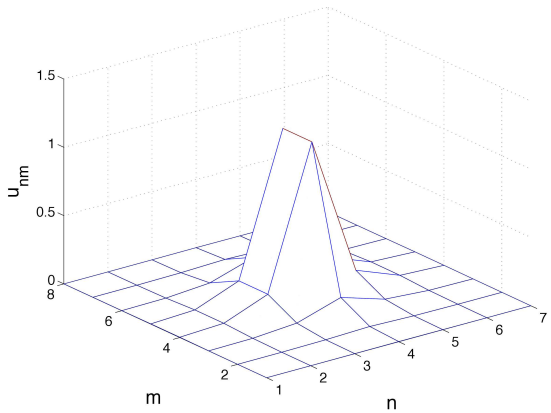

hybrid

Digression into 2D

- Snaking of bond-centred states for $C^+ = 0.1$, $C^\times = 0$:

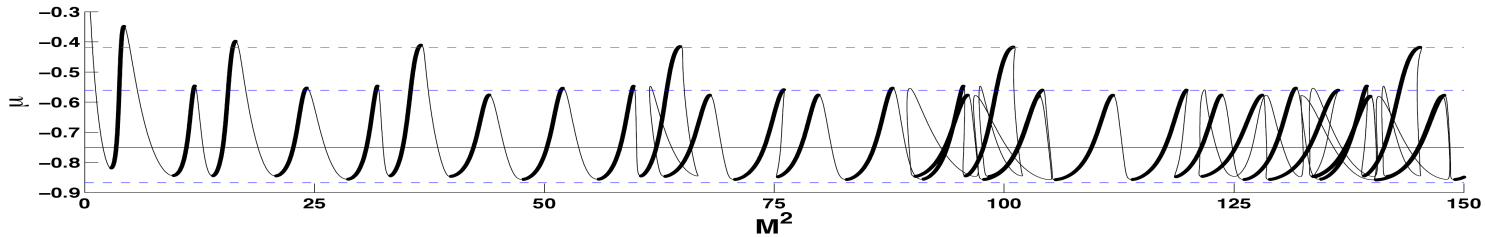

- Snaking of bond-centred states for $C^+ = 0.2$, $C^\times = 0$:

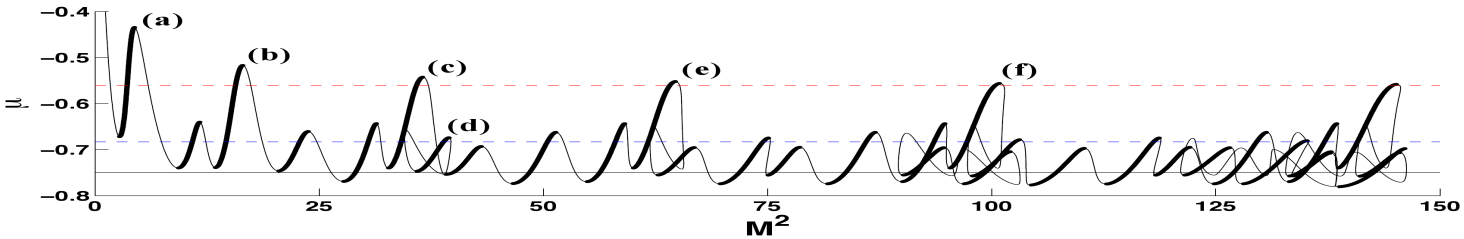

- Lines are predictions from 1D fronts: red–along lattice; blue–diagonal.

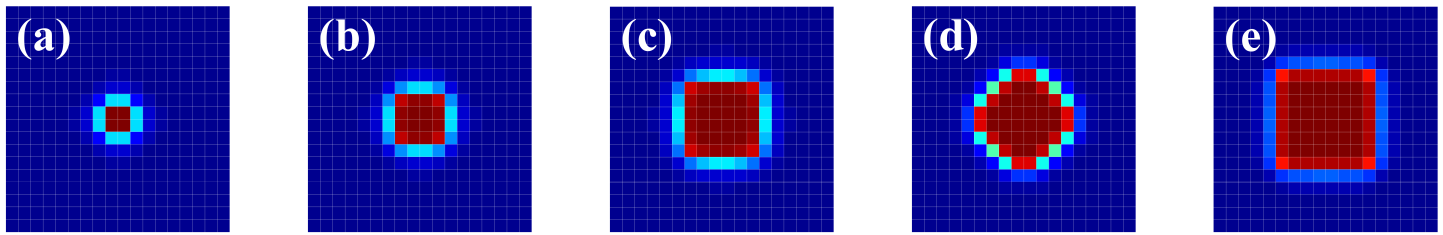

C.R.N. Taylor & J.H.P. Dawes, Snaking and isolas of localized states in bistable discrete lattices. Preprint (2009)

Digression: isolas and switchbacks

- Isolas exist at small C^+ and collide with the snake to form downward twists – 'switchbacks'; $C^+ = 0.19, 0.21$:

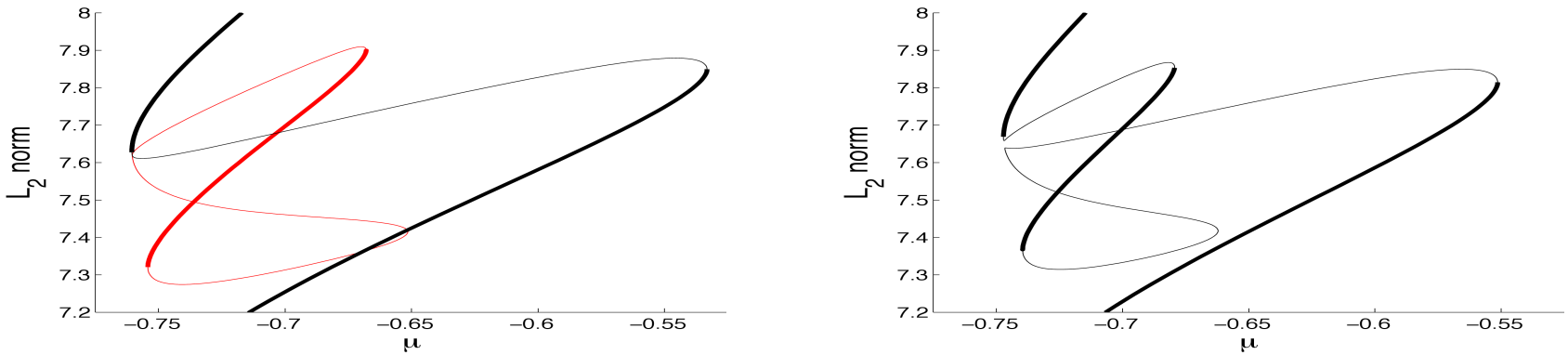

- ...and then detach from snake as C^+ increases further; $C^+ = 0.27, 0.28$:

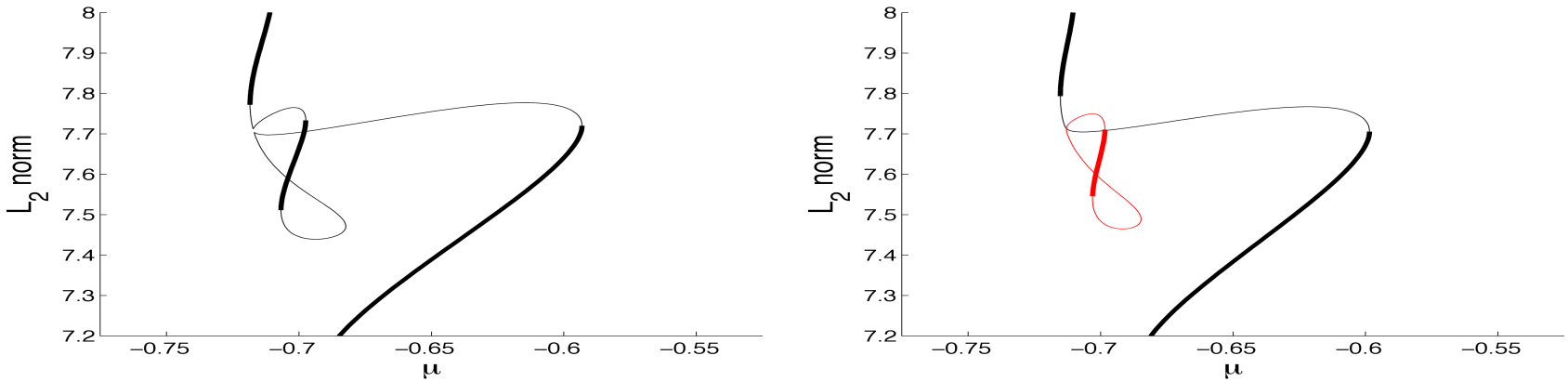

- Attachment/detachment occurs over very small intervals in C^+, $\sim 10^{-3}$.

Part III
From discrete to continuous

From discrete to continuous

- Is there any connection between discrete coupled-cell systems and PDEs such as Swift–Hohenberg?
- What is the 'continuum limit' of the coupled-cell system?

$$\dot{u}_n = C(u_{n+1} - 2u_n + u_{n-1}) + \mu u_n + 2su_n^3 - u_n^5$$

- Answer:

(1) $$u_t = u_{xx} + \mu u + 2su^3 - u^5$$

- i.e. no snaking!
- But is it possible to capture some 'leading-order correction' to (1) that sheds light on the limiting process $C^{-1} \equiv h^2 \to 0$ and shows how the snaking disappears?
- Need to examine some kind of long-wavelength approximation

P.G. Kevrekidis, I.G. Kevrekidis, A.R. Bishop & E.S. Titi, *Phys. Rev.* E **65**, 046613 (2002)
P. Rosenau, *Phys. Lett.* A **311**, 39–52 (2003) ; *Phys. Rev.* B **36**, 5868–5876 (1987)

Well, maybe

First guess (not so good), Taylor expansions:

- Suppose there exists a continuum field $u(x,t)$ such that $u(nh,t) = u_n(t)$. Then we have ($' \equiv p/\partial z$):

$$u_{n+1} = u_n + hu'_n + \frac{h^2}{2}u''_n + \frac{h^3}{6}u'''_n + \frac{h^4}{24}u^{(4)}_n + O(h^5)$$

$$u_{n-1} = u_n - hu'_n + \frac{h^2}{2}u''_n - \frac{h^3}{6}u'''_n + \frac{h^4}{24}u^{(4)}_n + O(h^5)$$

- which implies

$$h^{-2}(u_{n+1} - 2u_n + u_{n-1}) = u''_n + \frac{h^2}{12}u^{(4)}_n + O(h^3)$$

- So the PDE to this order is

$$u_t = u_{xx} + \frac{h^2}{12}u_{xxxx} + \mu u + 2su^3 - u^5$$

Dispersion relations

$$u_t = u_{xx} + \frac{h^2}{12} u_{xxxx} + \mu u + 2su^3 - u^5$$

- This PDE is ill-posed because high wavenumbers grow unboundedly!

Linearise, put $u \sim \mathrm{e}^{\sigma t + \mathrm{i}kx}$:

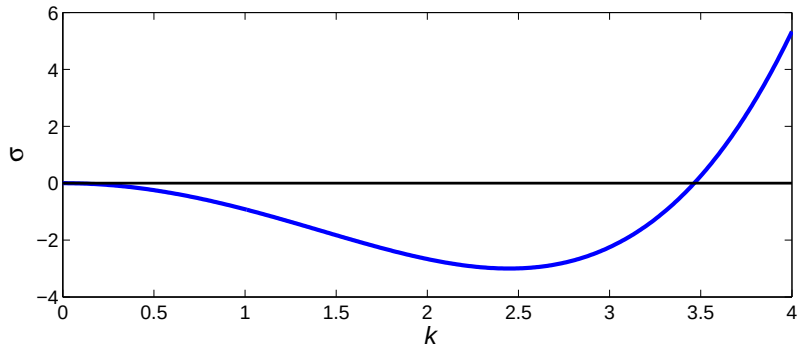

- Include 6th order Taylor series term:

$$u_t = u_{xx} + \frac{h^2}{12} u_{xxxx} + \frac{h^4}{360} u^{(6)} + \mu u + 2su^3 - u^5$$

dashed: $h = 0.1$

solid: $h = 10.0$

Nothing qualitatively new compared to 2nd order eqn

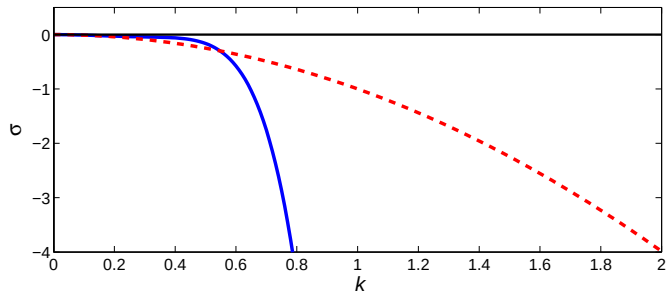

Full dispersion relation

- Note that, from the Taylor series arguments we have

$$\begin{aligned} u_{n+1} \equiv u(nh+h) &= \exp(hD)u_n \\ u_{n-1} \equiv u(nh-h) &= \exp(-hD)u_n \end{aligned}$$

where $D \equiv \partial/\partial z$,

- so that

$$h^{-2}(u_{n+1} - 2u_n + u_{n-1}) = \frac{2}{h^2}\left(\cosh(hD) - 1\right)u_n =: L(D)u_n.$$

- Now, Fourier transforming by sending $D \to \mathrm{i}k$, we have

$$\partial_t \hat{u}(k,t) = \hat{L}(k)\hat{u}(k,t) + \hat{F}(u)$$

where

$$\boxed{\hat{L}(k) = -\tfrac{4}{h^2}\sin^2\left(\tfrac{hk}{2}\right)}$$

Full dispersion relation

$$\hat{L}(k) = -\frac{4}{h^2}\sin^2\left(\frac{hk}{2}\right)$$

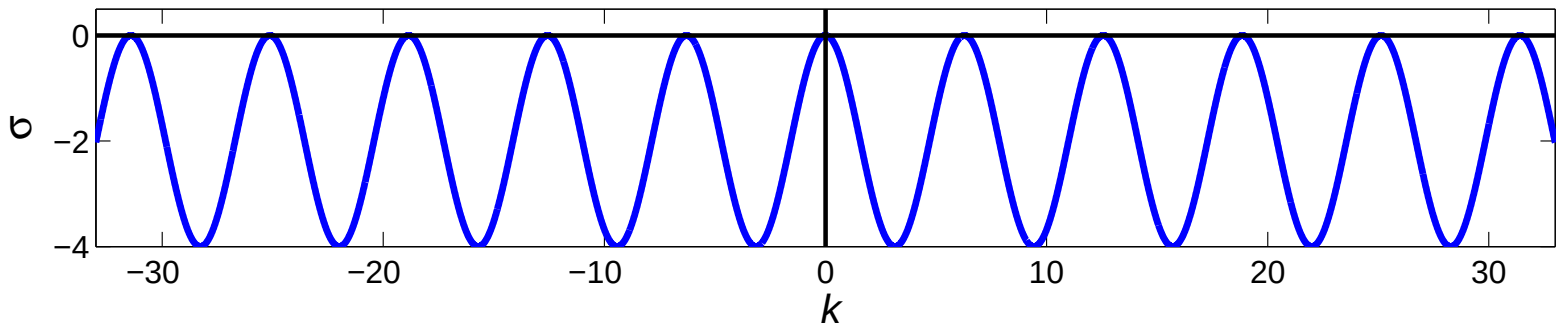

- $\hat{L}(k)$ is a pseudo-differential operator.
- Attempt to simplify to a PDE by finding rational or polynomial approximations for small $|k|$.
- 2 obvious kinds of approximation
  - Padé approximants
  - Weierstrass product representation

Padé approximants

- Lowest-order Padé approximants $(2p, 2q)$ to $\sin^2(x)$ are

$$P_{(2,2)}(x) = \frac{x^2}{1 + x^2/3}$$

$$P_{(4,2)}(x) = \frac{x^2 - x^4/5}{1 + \frac{2}{15}x^2}$$

$$P_{(4,4)}(x) = \frac{x^2 - \frac{10}{63}x^4}{1 + \frac{11}{63}x^2 + \frac{13}{945}x^4}$$

$$P_{(6,2)}(x) = \frac{x^2 - \frac{11}{42}x^4 + \frac{13}{630}x^6}{1 + \frac{1}{14}x^2}$$

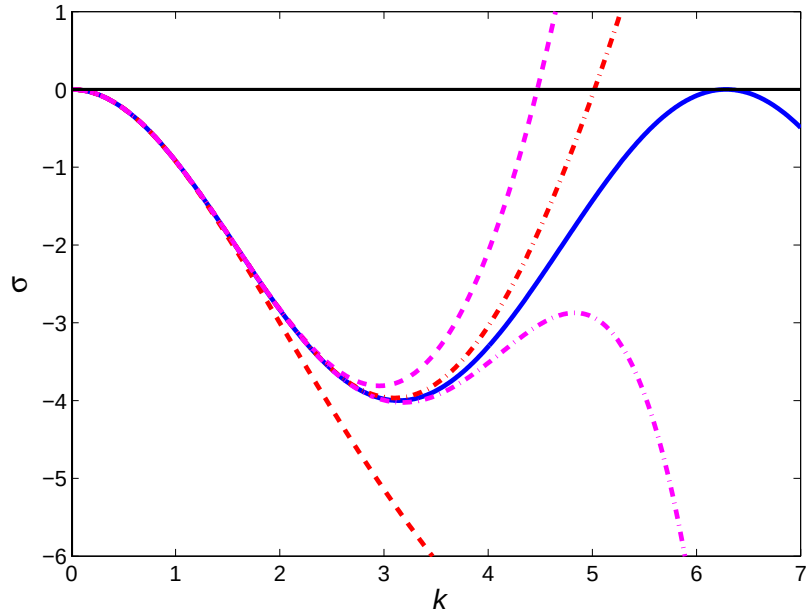

- Plot shows $\sigma = \mu - 4/h^2 P_{(2p,2q)}(hk/2)$ for $\mu = 0$, $h = 1$.
- None of these capture turning point at $k = 2\pi/h$ well.

Weierstrass product

Recall the infinite product representation of $\sin$:

$$\hat{L}(k) = -\frac{4}{h^2}\sin^2\left(\frac{hk}{2}\right) = -k^2\prod_{n=1}^{\infty}\left[1-\left(\frac{hk}{2\pi n}\right)^2\right]^2$$

leads to the 6th order approximation given by keeping only the $n=1$ term:

$$\hat{L}_1(k) := -k^2\left[1-\left(\frac{hk}{2\pi}\right)^2\right]^2$$

only the $n=1$ term:

only the $n=1$ and $n=2$ terms:

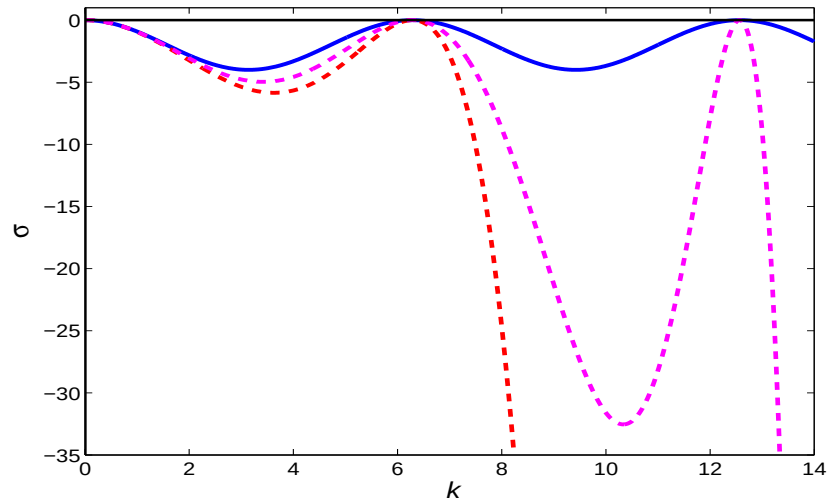

PDE approximation

- Turn $\hat{L}_1(k)$ back into a PDE:

$$u_t = \left[1 + \left(\frac{h}{2\pi}\right)^2 \frac{\partial^2}{\partial x^2}\right]^2 u_{xx} + \mu u + 2su^3 - u^5$$

- 'Swift–Hohenberg plus 2 more derivatives'.
- Let $d = h/(2\pi)$ for convenience.

Properties of this PDE:

- Limit $d \to 0$ is singular.
- d can be set to 1 by the useful rescaling:

$$\mu = \tilde{\mu} d^{-2}, \qquad s = \tilde{s} d^{-1}, \qquad u = \tilde{u} d^{-1/2}, \qquad t = \tilde{T} d^2, \qquad x = \tilde{X} d$$

- First integral (let $F(u) = \frac{\mu}{2}u^2 + \frac{s}{2}u^4 - \frac{1}{6}u^6$):

$$H = \frac{1}{2}(u_x)^2 + 2d^2\left(u^{(3)}u_x - \frac{1}{2}(u_{xx})^2\right) + d^4\left(u^{(5)}u_x - u^{(4)}u_{xx} + \frac{1}{2}\left(u^{(3)}\right)^2\right) + F(u)$$

Weakly nonlinear analysis

- Neutral modes at $k = 0$ and $k = 2\pi$ suggest a mode interaction.
- Usual multiple-scales expansion for small amplitude, mildly subcritical instabilities:

$$u = \varepsilon \left(A(X,T) + B(X,T)\mathrm{e}^{\mathrm{i}x} + c.c. \right) + \varepsilon^2 u_2 + \cdots$$

where

$$\mu = \varepsilon^4 \tilde{\mu}, \qquad s = \varepsilon^2 \tilde{s}, \qquad T = \varepsilon^4 t, \qquad X = \varepsilon^2 x$$

gives, at $O(\varepsilon^5)$, a pair of amplitude equations for A, B (now assumed real):

$$\begin{aligned} A_T &= A_{XX} + \mu A + 2sA^3 - A^5 + 12sAB^2 - 20A^3B^2 - 30AB^4 \\ B_T &= 4B_{XX} + \mu B + 12sB^3 - 20B^5 + 12sBA^2 - 10BA^4 - 60B^3A^2 \end{aligned}$$

Weakly nonlinear analysis

Three kinds of constant solution:

- $A \neq 0$, $B = 0$: flat homogeneous state
- $B \neq 0$, $A = 0$: periodic pattern - 'discretisation effect'
- $AB \neq 0$: mixed mode

On constant solutions the first integral becomes (at this order)

$$H = \frac{\mu}{2}A^2 + \frac{s}{2}A^4 - \frac{1}{6}A^6 + \mu B^2 + 3sB^4 - \frac{10}{3}B^6 + 6sA^2B^2 - 5A^4B^2 - 15A^2B^4$$

Maxwell points of equal H on the different constant solution branches exist:

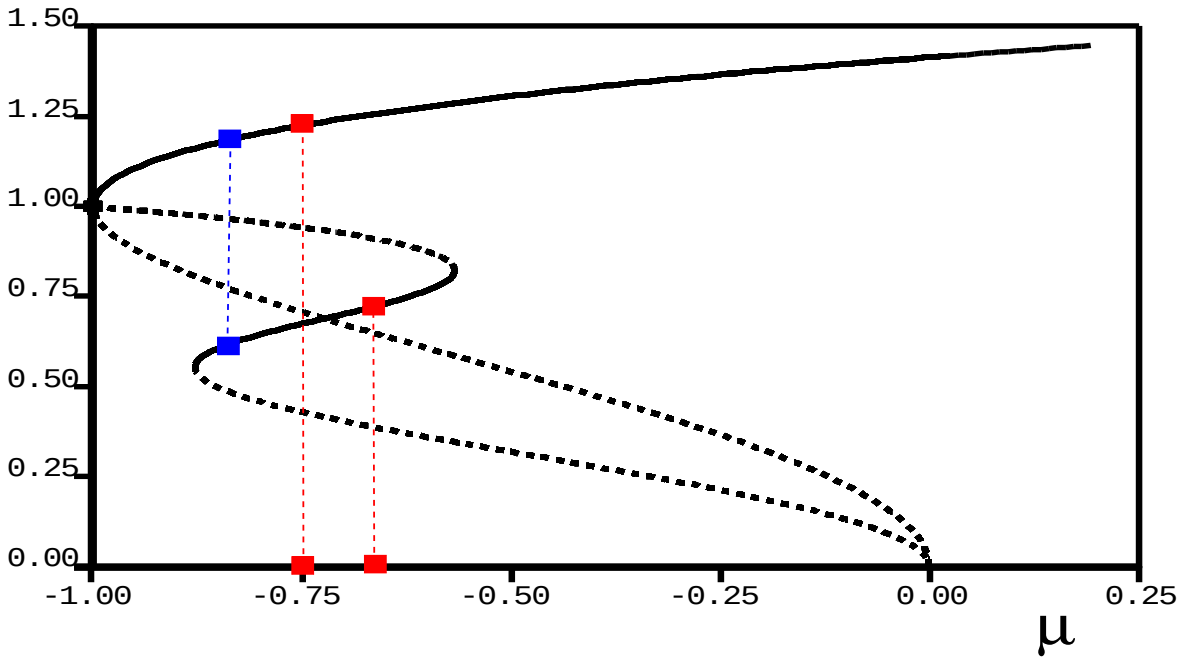

Fronts near the Maxwell points

Three kinds of fronts:

- zero–mixed mode (a below)
- mixed-mode–flat (c below)
- zero–flat: not shown, but 'as normal', as in the 2nd order ODE obtained when $d = 0$.

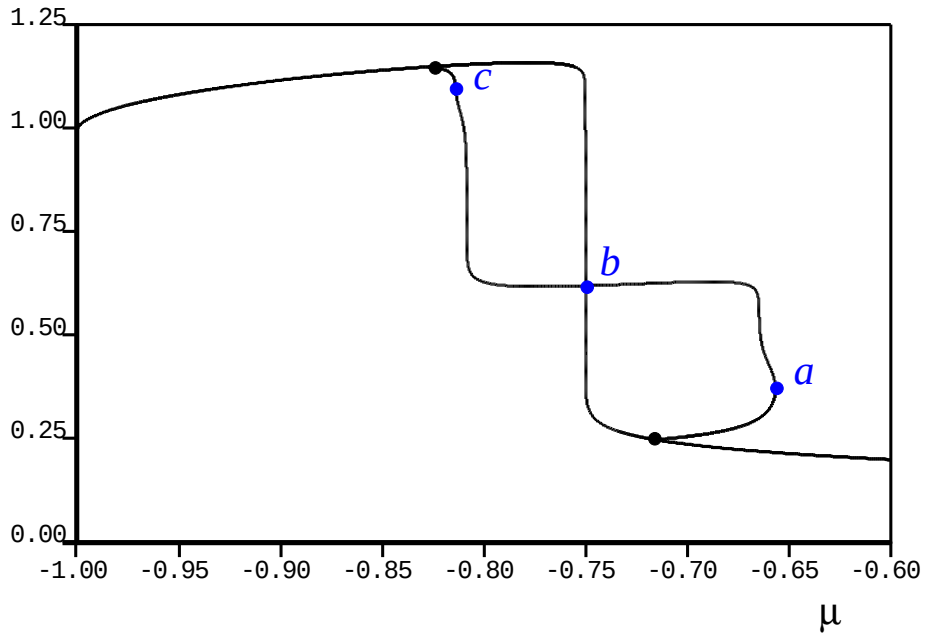

$A(X)$ - solid; $B(X)$- dashed; $A + 2B\cos x$ - dash-dotted:

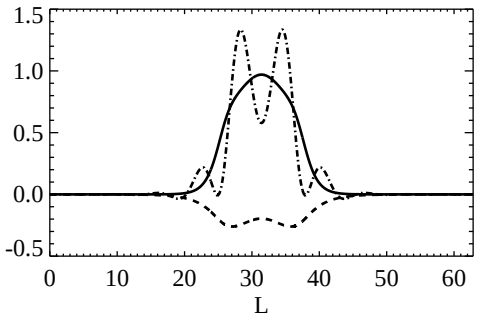

(a)

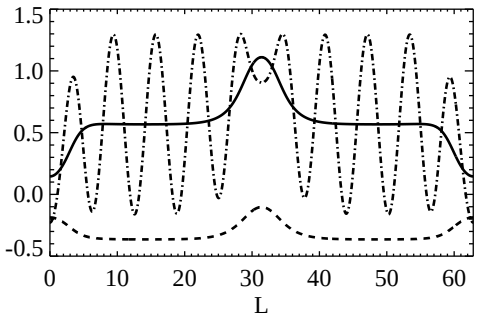

(b)

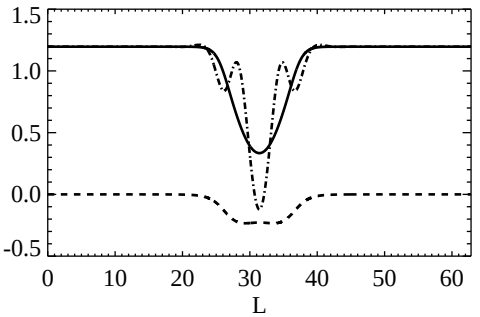

(c)

Snaking 1/2

Two (halves of) fat snakes twist around the

- zero–mixed-mode, and
- flat–mixed-mode

Maxwell points

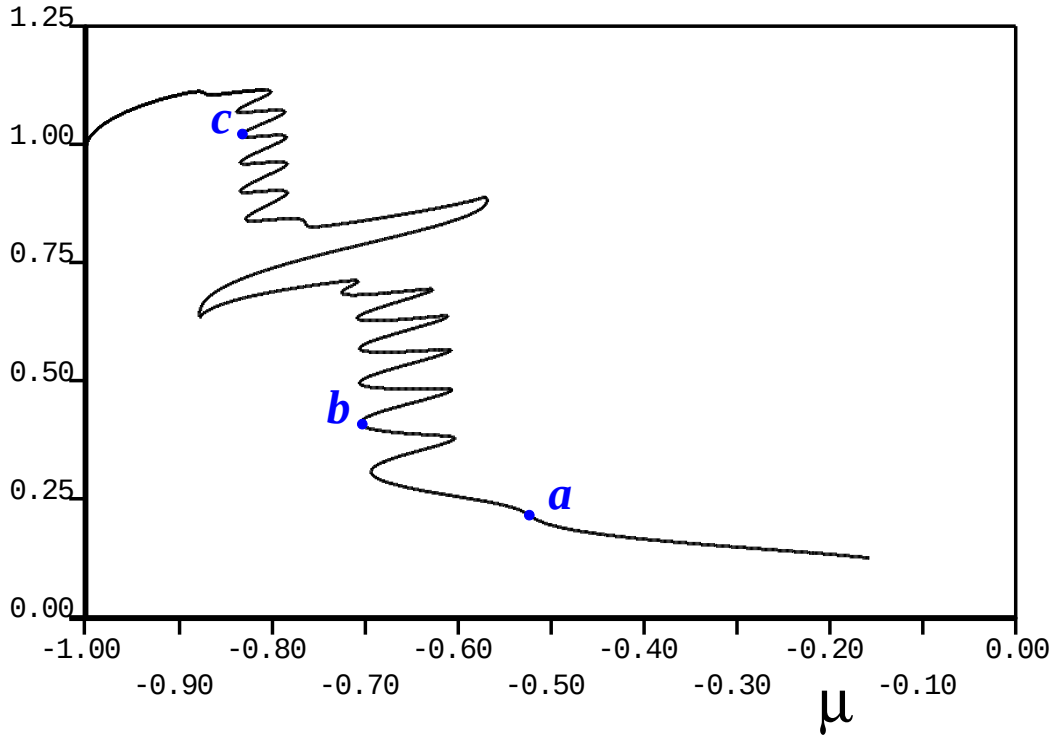

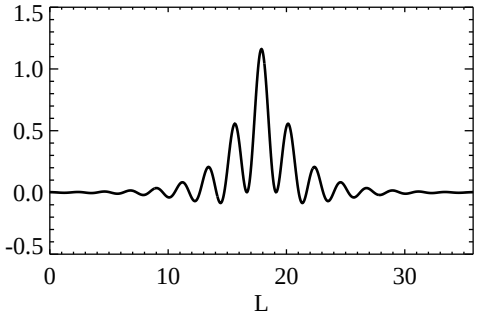

(a)

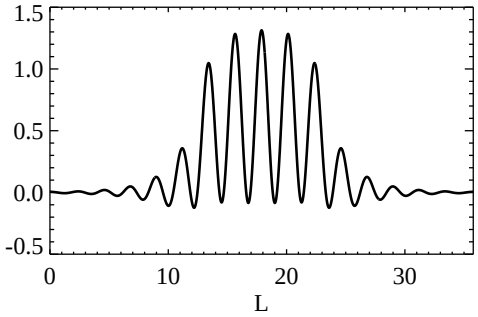

(b)

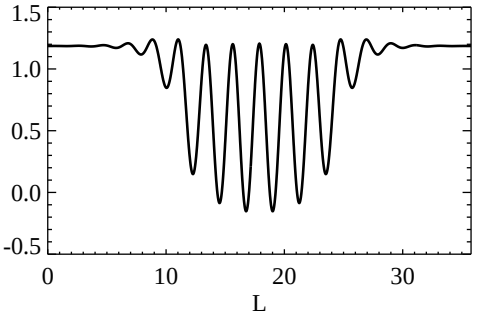

(c)

Snaking 2/2

Snake around the zero–flat Maxwell point is ‘thin’:

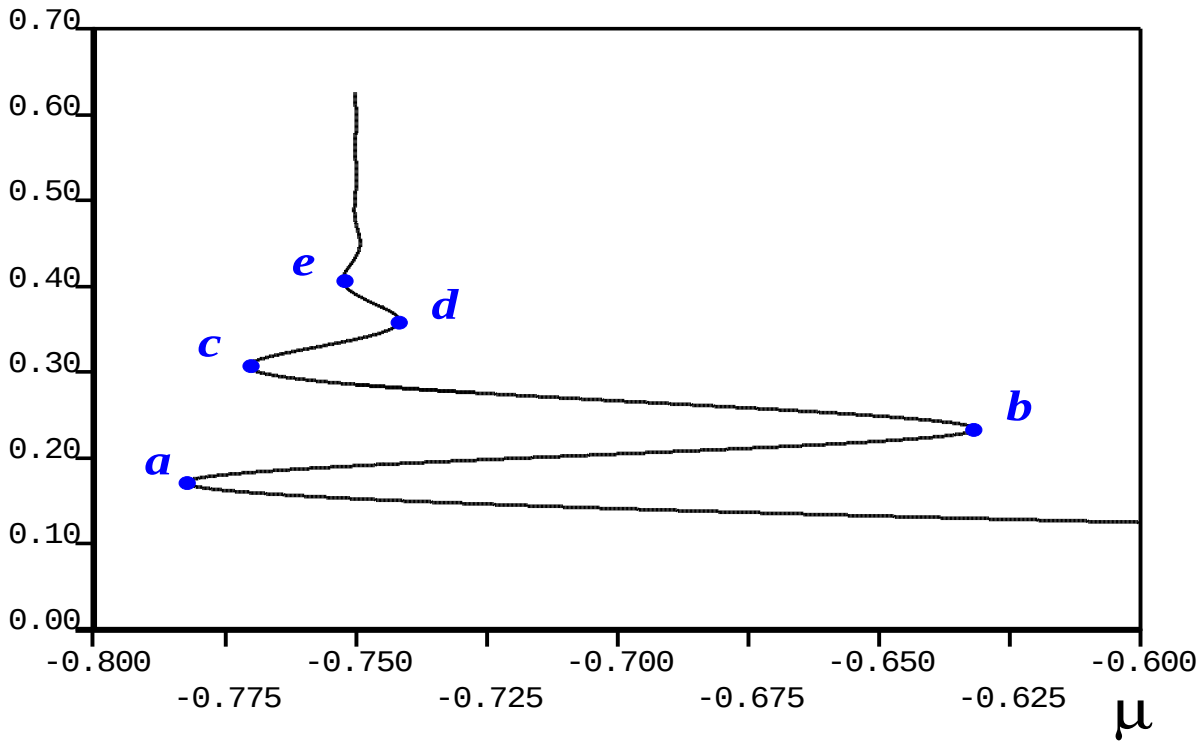

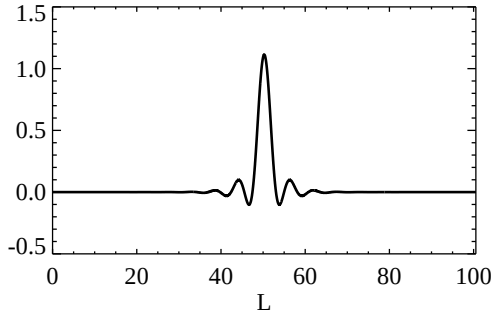

(a)

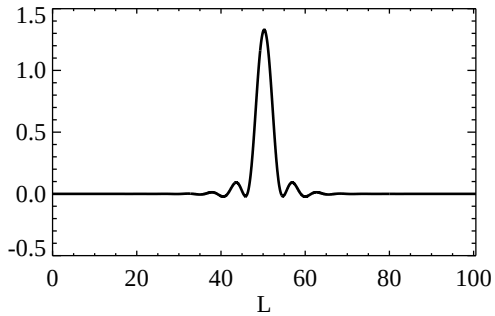

(b)

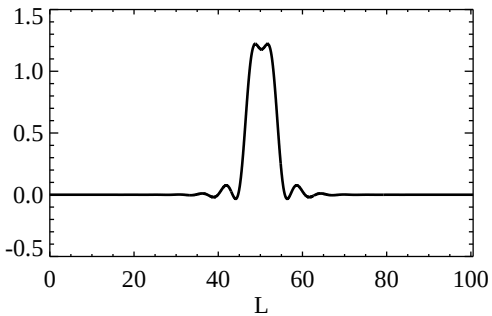

(c)

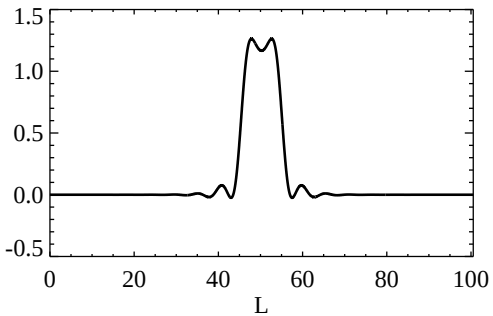

(d)

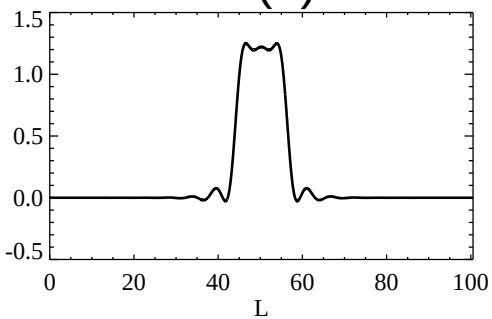

(e)

Varying d in a finite domain

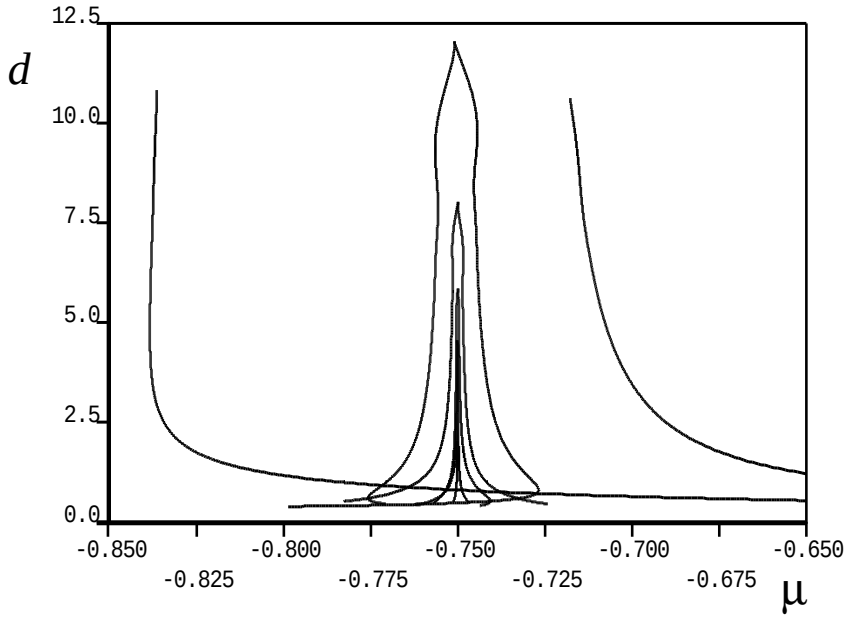

- As d increases
  - twists pinch-off in saddle-node bifurcations
  - We return to the monotonic front of the 2nd order 'limiting case'
- As d decreases, snake broadens rapidly

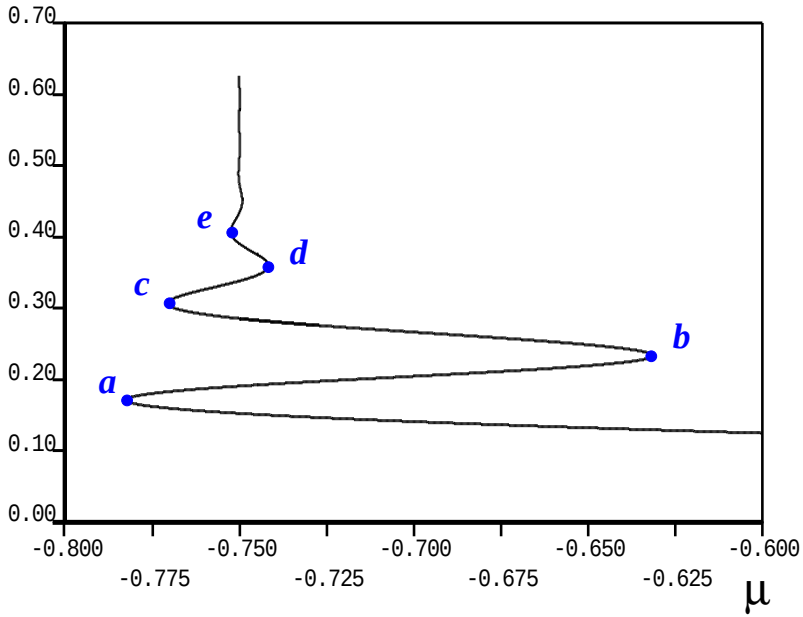

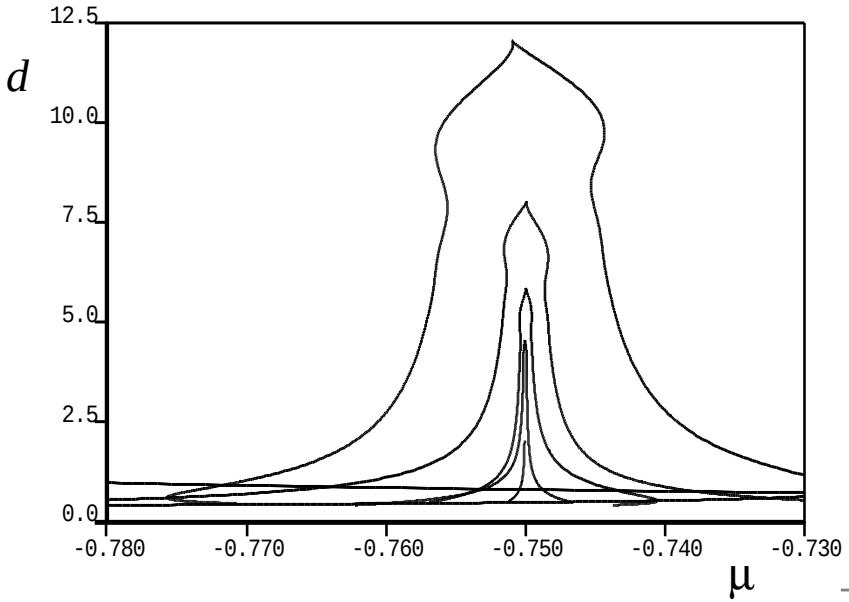

Summary

- An additional large-scale mode reinforces the existence of stable (1D) localised states. Novel analysis in the limit $\zeta \ll 1$.
- Many similarities exist between snaking in continuum systems such as Swift–Hohenberg and discrete systems.
- Lots to be done in 2D (and 3D!) still.
- Continuum limit is problematic and singular
  - Nice 6th order model equation that preserves variational structure
  - In a finite domain, 6th order model equation provides a smooth path back to the 2nd order equation as $d \to \infty$ (!!??) and the discretisation effects 'wash out' to scales larger than the domain.